iJERGS International Journal of Engineering Research And General Science

Journal which deals with research, Innovation and Originality

International Journal Of Engineering Research and General Science

ISSN 2091 - 2730

Table of Content

CHIEF EDITOR BOARD

Message from IJERGS

This is the Sixth Issue of the Fifth Volume of International Journal of Engineering Research and General Science. A total of 6 research articles are published and we sincerely hope that each one of these provides some significant stimulation to a reasonable segment of our community of readers.

In this issue, we have focused mainly on the Scholars approach for innovation. We also welcome more research oriented ideas in our upcoming Issues.

Author's response for this issue was really inspiring for us. We received many papers from many countries in this issue but our technical team and editor members accepted very less number of research papers for the publication. We have provided editors feedback for every rejected as well as accepted paper so that authors can work out in the weakness more and we shall accept the paper in near future.

Our team have done good job however, this issue may possibly have some drawbacks, and therefore, constructive suggestions for further improvement shall be warmly welcomed.

IJERGS Team,

International Journal of Engineering Research and General Science

E-mail – feedback@ijergs.org

International Journal of Engineering Research and General Science Volume 5, Issue 6, November-December, 2017
ISSN 2091-2730

Overview of Automotive Seating System

Amit Patil[1] , Utkarsh Patil[2]

[1]Graduated student, MIT College of Engineering, Pune

[2]Student, Department of mechanical Engineering, MIT College of engineering Pune

amitpatil050@gmail.com

Abstract:-In Automobiles, Seat is very important part. The standard car seat is designed to support thighs, the buttocks, lower and upper back, and head support. The front driver and passenger seats of most vehicles have three main parts: the seat back (squab), seat base (cushion), and the head-rest. These components are usually constructed from foam to provide comfort to the rider. When choosing this product, foam manufacturers must consider the most suitable foam for balancing comfort, support, safety, and recycling properties. This paper gives overall idea of Automotive seating system.

Keywords— Automobile, Seat, Head rest, Foam, Tracks, Recliners, Seat belt.

INTRODUCTION

Automotive seat is used to give comfort to the person who is driving. The cushioning agent is especially important when considering that moving cars can transmit vibrations near the human spine's resonant frequency of 3 Hz. The base can usually be moved forward and back on metal railings and may move up and down to adjust to different body types. This movement is accomplished either by manual latches or by electric levers. Now we will see the entire Seating System.

MAIN FUNCTION OF SEAT:-

Seat system is the very important part of the vehicle which always comes in contact with the occupant when the vehicle is used and is also directly responsible for the comfort/safety of the occupant.

1. Occupant Support:-

    a. Occupant should get stable support for long time.

    b. Occupants of various weights, sizes and proportions should be accommodated in the Seat.

2. Occupant Position:-

    a. Occupant position is very important for safe operation of the vehicle.

    b. Occupant should be positioned ergonomically so as to have clear field of vision.

    c. Occupant should have good Head, leg and arm room.

3. Protect Occupant:-

    a. During the crash occupant should not be unduly displaced from the seat.

    b. Seat system parts should not injure occupant before/during/after vehicle crash.

Main assemblies / areas within the Seat (CAD):-

The automotive seating system consist of following parts:-

1. **Head Rest:-**

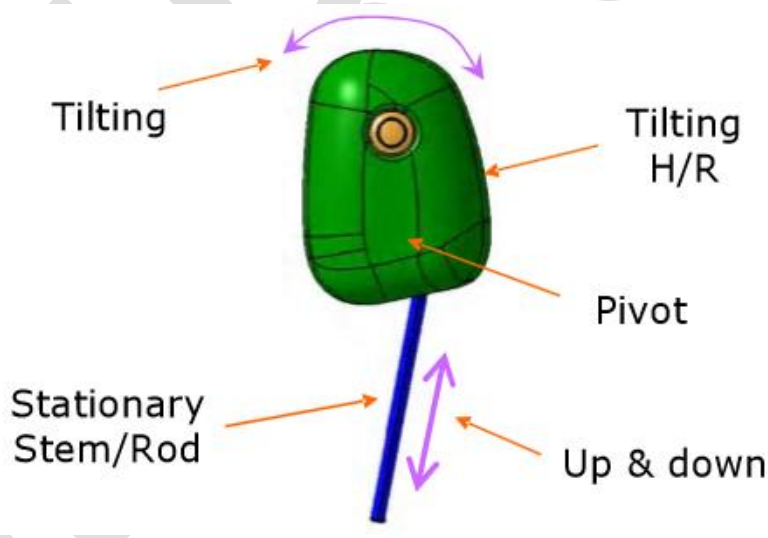

In most cars head restraints are kept relatively small in order not to unnecessarily obstruct the rear passenger visibility. Two seater sports cars often have a much larger head restraint area which is safer. A small head restraint has to be adjustable for the user and some are also adjustable in angle as if they might be used as a head rest. An effective comfortable head rest, as for instance on a fireside chair, has to support the base of the skull near the top of the neck. This would be extremely dangerous in a car. It is this confusion and the simple fact that what can be adjusted right will usually be adjusted wrong that led Design to avoid any adjustment in head rests.

FUNCTION OF HEAD REST:-

1. Prevents head injury during vehicle crash.
2. Supports head.
3. DVD/VCD screen can be packaged in Head rest.

TYPES OF HEAD REST DEPENDING UPON SAFETY:-

1. Active – Activates during vehicle crash.
2. .Passive – Does not activates during crash.

STANDARD MATERIAL USED IN HEAD REST:-

1. Head rest structure (Rod/Stem).
2. Plastic
3. Foam.
4. Trim.

HEAD REST CONFIGURATIONS:-

1. Can move up and down.
2. Can rotate (Tilt) along the pivot in forward and rearward direction.
3. Wings on the Head restraint can rotate and support head.
   (Head rest can be 2-Way, 4-Way and 6-Way depending upon above combination)

2. Seat Back :-

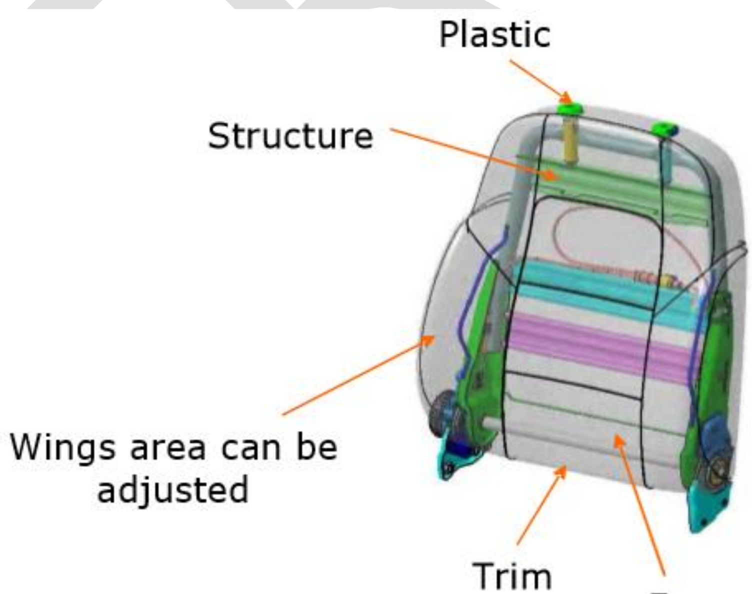

Seat back assembly mainly consist of 4 parts as shown in the picture above. It is very important in order to have comfortlness to the occupant

FUNCTION OF SEAT BACK :-

1. Supports occupant's back.
2. Positions occupant's back.

International Journal of Engineering Research and General Science Volume 5, Issue 6, November-December, 2017
ISSN 2091-2730

Standard seat back assembly consists of

1. Metal structure.
2. Plastic
3. Foam
4. Trim

There are a lot of features which are incorporated within the seat back assembly. Lumber support is one feature. Back of seat is so designed to have enough lumber support. In some cases it is also used as the heating and ventilation purpose. Folding pad, Lap top tray, Side Air bag, Knee air bag for Rear seat occupant are some of the important features.

3. **Seat Cushion:-**

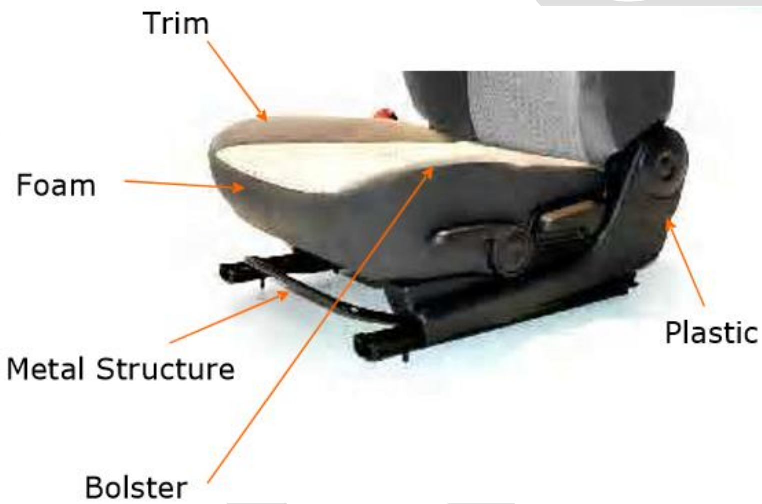

Seat cushion is important in order to get the thighs support and position of occupants. During the manufacturing of seat cushions polyethers are used.

FUNCTION OF SEAT CUSHION:-

1. Supports occupant ischium and thighs.
2. Positions occupant.

Standard Seat Cushion assembly consists of

1. Metal structure.
2. Plastic
3. Foam.
4. Trim.

SEAT CUSHION CONFIGURATIONS:-

1. Can move in forward and rearward direction.
2. Can move up and down (Height adjustment).
3. Can tilt (Thigh support)
4. The Bolster can rotate.

5. **SEAT BELT:-**

In a severe collision, the occupant can either strike the dashboard, or strike the seat belt. How much trauma the body of the occupant experiences will depend on the time period over which the force is applied and the stiffness of the body parts absorbing the force. Stretching the time epoch of the collision for the occupants and redistributing the crash forces to the stiffest parts of the human anatomy is the duty of the seat belt. Equally important, seat belts are the best way to prevent ejection from the vehicle.
The seat belt restraint system contains some or all of these components

1. shoulder guide loop,
2. webbing
3. non-locking retractor
4. automatic locking retractor
5. emergency locking retractor
6. vehicle sensitive retractors
7. webbing sensitive retractors
8. buckle
9. buckle release
10. tongue (latch plate)
11. selvage

6. **AIRBAGS:-**

All cars feature dual-stage front airbags as well as front side-impact and side curtain airbags, controlled by a "smart" airbag system that detects passenger weight, seatbelt use and driver's seat position, then deploys the front airbags accordingly while ensuring the side-impact and side curtain airbags only deploy when needed. The dual-stage means they can be deployed in one of two ways: a low to medium speed collision will cause a single-stage deployment, while a severe impact will trigger a full deployment. The front side-impact airbags are built right into the front seats to ensure they are in proper position at all times. The side curtain airbags deploy from above the side windows to almost completely cover the front and rear side windows and the center pillar, helping to protect against injury and intrusions into the cabin in a side impact.

MECHANISMS USED IN THE SEATS:-

1. Recliners:-

FUNCTION OF RECLINER:-

- Allow to tilt Seat back in forward and rearward direction by specified angle.

Selection of recliner depends upon following factors:-

1. Safety and regulation – The load which Recliner is going to take
2. Manual / Power – It depends upon whether seat is luxurious or not.
3. Price
4. Continuous or discontinuous
5. Availability

2. Tracks:-

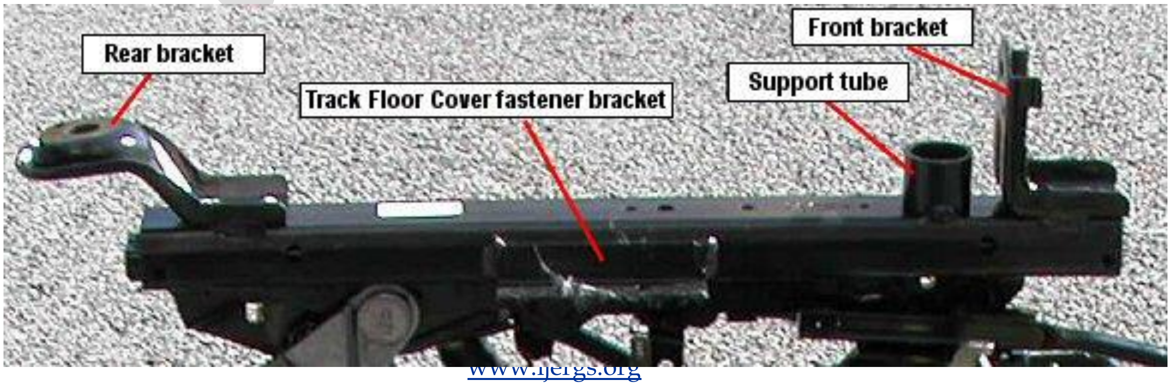

FUNCTION OF TRACKS:-

- The Function of track is to allow movement of Seat in forward and reverse direction by specified distance.

Selection of Track depends upon following factors –

1. Safety and regulation – The load which track going to take
2. Manual / Power – It depends upon whether seat is luxurious or not.
3. Price
4. Availability

3. Cushion height adjustment/tilt:-

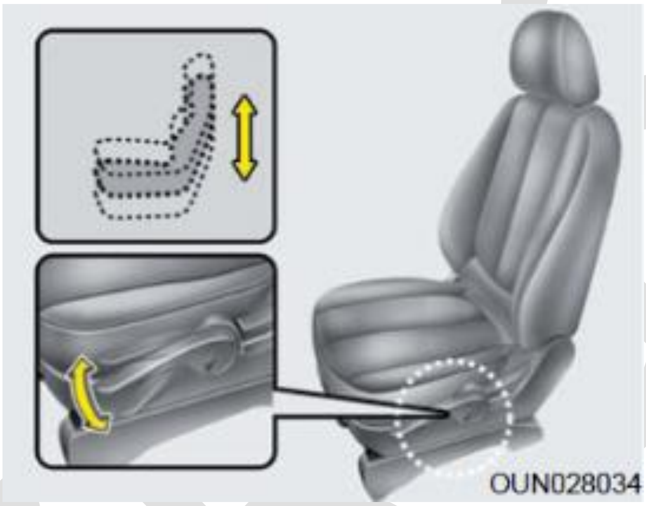

FUNCTION OF CUSHION HEIGHT ADJUSTMENT:-

- Allows to move Seat up and down direction by specified distance.

Selection of Track depends upon following factors –

1. Safety and regulation
2. Manual / Power – It depends upon whether seat is luxurious or not.
3. Price
4. Availability

FACTORS NEED TO BE CONSIDERED WHILE DESIGNING THE SEAT:-

1. **Sheet metal design:-**
   a. In most of the seats, sheet metal contribute more than 70% of weight, so it is important to understand sheet metal design thoroughly.
   b. One should know all the processes of the sheet metal – Blanking, piercing, Bending, Drawing, Deep drawing, hemming, Lancing, forming etc.
   c. The designer should understand the importance of part in terms of safety, support etc.
   d. Selection of material – It depends upon
      1. Yield stress.
      2. Thickness of the sheet.
      3. Availability in particular region.
      4. Cost.
   e. Process to manufacture –
      1. The designed Sheet metal part should have manufacturability.
      2. The cost for the tooling should be minimum.

2. **Tube Structure Design:-**
   a. Few of the seats are made up of tube structure. The tube may have circular, box type cross section.
   b. One should know the processes of the tube structure design – Bending, flattening etc.
   c. The designer should understand the importance of part in terms of safety, support etc.
   d. Selection of material – It depends upon
      1. Yield stress.
      2. Diameter/Thickness of the tube.
      3. Availability in particular region.
      4. Cost.
   e. Process to manufacture –
      1. The designed tube part should have manufacturability.
      2. The cost for the tooling should be minimum.

3. **Wire structure design:-**
   a. Mainly wire structure is used to give support to foam and trim. ISO fix and Top tether anchorages are made up of wires.
   b. One should know the processes of the wire structure design – Mainly bending
   c. The designer should understand the importance of part in terms of safety, support etc.

4. **Foam Design**:–
   a. Foam is designed by considering A-surface and structure of the seat.
   b. Design of the foam directly affects the comfort of the occupant.

5. **Trimming consideration:**– It mainly deals with the craftsmanship issues

6. **Plastics: -** It mainly deals with the craftsmanship issues and covers the metal structure.

7. **Joints:-**
   a. Welding - CO_2/Gas metal arc welding, spot welding are generally used in Seating. Welding length, welding overlapping of two parts need to be considered.
   b. Bolting - Selection of particular bolt size for required application is important. E.g. Cushion and Back marriage bolts should be minimum of size M10, Self tapping screws like M4 are used to attach plastic part to Seat.
   c. Rivet - At few places riveting is used as a joint.
   d. Free pivot – Free pivot is used where the joint is required but two parts needs to rotate freely with respect to each other

8. **Assembly sequence:-**
   a. By understanding assembling sequence different assemblies and sub-assemblies are created.
   b. Generally following is the assembly sequence – Welded parts-Bolted/riveted/free pivot parts-foam-Trim- Plastic
   c. JIT line will have different assembly sequence.

9. **Assembly/Part drawing**:-
   a. Every drawing should have all the important dimensions with GD & T.
   b. Drawing should be made in specific Template e.g. Nissan will have Nissan template.
   c. If required, BOM, welding information, Torque table etc. should be provided.
   d. Tolerance stack up is done where ever required.

10. **Packaging**:–
    a. During the packaging of the Seat in Vehicle environment or individual component of seat with in seat, kinematics of the seat or part should be done to check the interference.
    b. Tool runner access and welding gun access should be checked.
    c. Meat to metal should be checked between Manikin and Seat Hard points.

CONCLUSION:-

In conclusion according to the above information should be considered while designing the seat. It gives the information about different parts of seat which will surely helpful to the designer.

REFERENCES:

[1] Mohamad,D., Deros,B.M., Wahab,D.A., Daruis,D.D.I., & Ismail,A.R., 2010, "Inegration of Comfort into a Driver's car Seat Design Using Image Analysis", American Journal of Applied Sciences, (7) 937-942

[2] Runkle, V.A., “Benchmarking Seat Comfort”, Society of Automotive Engineers, Inc., Warrendale, PA, USA, 1994, SAE Technical Paper No. 940217.

[3] Hertzberg, H.T.E. 1972, “The Human Buttocks in Sitting: Pressures, Patterns, and Palliatives”, Society of Automotive Engineers, Inc., New York, NY, USA, 1972, SAE Technical Paper no. 72005.

[4] Shen, W. and Parsons, K.C., “Validity and Reliability of Rating Scales for Seated Pressure Discomfort”, International Journal of Industrial Ergonomics, Vol. 20, 1997, pp. 441-461.

[5] De Looze, M. P., Kuijt_Evers, L. F. M. and Dieen, J. V., “Sitting Comfort and Discomfort and the Relationship with Objective Measures” Ergonomics, Vol. 46, No. 10, 2003, pp. 985-997.

[6] Mohd. Tamrin, S.B., Yokoyama, K., Jalaludin, J., Abdul Aziz, N., Jemoin, N., Nordin, R., Li Naing, A., Abdullah, Y., and Abdullah, M., “The association between risk factors and low back pain among commercial vehicle drivers in Peninsular Malaysia: A Preliminary Result”, Industrial Health, Vol. 45, 2007, pp. 268-278.

[7] De Looze, M. P., Kuijt_Evers, L. F. M. and Dieen, J. V., “Sitting Comfort and Discomfort and the Relationship with Objective Measures” Ergonomics, Vol. 46, No. 10, 2003, pp. 985-997.

[8] Dhingra, H. S., Tewari, V. K., and Singh, S., Discomfort, pressure distribution and safety in operator's seat- a critical review," Agricultural Engineering International: the GIGR Journal of Scientific Research and Development. Invited overview paper. Vol. V, 2003.

[9] Hinz, B., Rutzel, S., Bluthner, R., Menzel, G., Wolfel, H. P., and Seidel, H. “Apparent mass of seated man- first determination with a soft seat and dynamic seat pressure distributions”, Journal of Sound and Vibration, Vol. 298, 2006, pp. 704-724.

[10] Inagaki, H., Taguchi, T., Yasuda, E., and Iizuka, Y., “Evaluation of Riding Comfort: From the Viewpoint of Interaction of Human Body and Seat for Static, Dynamic, Long Time Driving”, Society of Automotive Engineers. Inc., Warrendale, PA, USA, 2000, Technical Paper No. 2000- 01-0643.

[11] Parakkat, J., Pallettiere, J., Reynolds, D., Sasidharan, M., and El-Zoghb, M., “Quatitative methods for determining U.S. Air Force crew cushion comfort”, Society of Automotive Engineers, Inc., Warrendale, PA, USA, 2006, Technical Paper No. 2006-01-2339

Optimization of Process parameters for Laser Fiber micromachining of micro – channels on Stainless Steel

Ramendra Singh Niranjan[1], Onkar Singh[2], J. Ramkumar[3]

[1]Assistant Professor, Department of Mechanical Engineering UIET CSJMU, Kanpur (India)

[2]Professor, Department of Mechanical Engineering HBTU, Kanpur (India)

[3]Professor, Department of Mechanical Engineering IIT, Kanpur (India)

[1]ramendrasingh@rediffmail.com, ramendra@uietkanpur.org

Abstract: Today Laser beam machining plays a very important role in the field of micro system technology. This work aims to show how the process parameters of laser Fiber Fusion engraving machine influence the final features of work- piece and also optimized the results through ANOVA software. Arrays of micro-channels were manufactured using various set of scanning speeds, pulse intensities and pulse frequencies. The results suggested that PF, PI and SS are the significant parameters in terms of depth and width of the channel which are the important for manufacturing in industry.

Keywords: Scanning Speed (SS), Pulse Frequency (PF), Pulse Intensity (PI), Micro-channels or Pin Fin.

1 Introduction

Laser beam machining is widely used in the field of micro system technology sectors, automotive manufacturing, diagnostic, medical applications, biomedicines, display units, printing technology etc. Developments in Fiber laser techniques (pulsed laser) and system has enhanced the applicability of laser in the complex component productions without expensive tooling. Machining of laser have wide range of materials such as metals and nonmetals, soft and difficult to machine. Pulsed lasers have more intensities than continuous wave lasers and are suited best solution for the fabrication of micro-channels or pin-fins structures. The Material removal during the laser machining process depends upon characteristics of the laser and the properties of the work-piece, Factors such that pulse frequency (PF), pulse intensity (PI), scanning speed (SS) and overlapping are influenced on laser and work-piece interaction. Many of these factors can be optimized in order to obtain the desire quality.

Various authors have investigated how laser parameters affect the resultant machined features. Teixidor et al 2013-[1] studied the capabilities of laser micro-machining by performing experiments on hardened steel with a pulsed Nd:YAG laser. Arrays of micro-channels were manufactured using various scanning speed, pulse intensities and pulse frequencies. The results are presented in terms of the main industrial requirements for nay manufactured good: dimensional accuracy (width and depth), surface roughness and material removal rate. E. V. Bordatchev et al 2003-[2] investigated experimentally the effect of laser pulse energy on the geometric quality of the machined parts in terms of accuracy, precision, and surface quality. They have experimentally formed the craters on thin copper foil with variation in laser pulse energy, the geometry and the surface topology. The geometrical parameters were measured and statistically analyzed with respect to incident pulse energy. Statistical analysis including pattern recognition was used to analyze the experimental data systematically and to serve proper selection of the process parameters to achieve the desired geometric quality of the machined parts. They have discussed the plausible trends in the crater geometry with respect to the laser pulse energy. Basem. F. Yousefa et al 2001-[3] described how an artificial neural network can be used to create a nonlinear model of the laser material-removal process in order to automate micro-machining tasks. The multilayered neural network was used to predict the pulse energy needed to create a crater of specific depth and average diameter. Laser pulses of different energy levels were impinged on the surface of the test material in order to investigate the effect of pulse energy on the resulting crater geometry and volume of material removed. They test the network's performance using experimentally acquired data from several sample materials. The experimentally acquired data demonstrates that the proposed network can simulate the behavior of the physical process to a high degree of accuracy. Kant Rishi et al 2014-[4], optimized the process parameter of laser micromachining technique which produce smooth machined surfaces. In addition, the impact of process parameters like raster speed, laser power, print resolution etc. were optimized using two target functions of dimensional precision and surface roughness. They analyzed the PMMA samples using 3D- profilometry and Field emission scanning electron microscope (FESEM) for surface quality and dimensional precision. Semaltianos et al 2010-[5] studied the effects of fluence and pulse frequency on surface roughness and MRR in nickel-based alloys with a Nd:YVO4 picosecond laser. They also analyzed the surface morophology of these alloys with AFM and SEM techniques.

Cadot et al 2016-[6] studied about the generation of controlled 3D micro-features by pulsed laser ablation in various materials. The key enabler of pulsed laser ablation for micro-machining was the prediction of the removal rate of the target material, thus allowing real-life machining to be simulated mathematically. Usually, the modeling of micro-machining by pulsed laser ablation is done using a pulse-by-pulse evaluation of the surface modification, which could lead to in accuracies when pulses overlap. To address these issues, a novel continuous evaluation of the surface modification that use trenches as a basic feature was presented in their work. The author investigated the accuracy of this innovative continuous modelling framework for micro-machining tasks on several materials.

Venkatakrishnan et al. 2002-[7] studied the laser micromachining on 1000 nm thick gold film using femstosecond laser. They found that during micromachining two ablation regimes exist. In the first regime no molten material is present and cutting is very shallow whereas in second regime the pulse energy is higher than ablation threshold and redeposition of molten material takes place. They suggested controlling the pulse energy in first ablation regime to get clean and precise microstructure. Similarly Venkatakrishnan et al.2002-[8] investigated the feasibility of sub-micron machining of metallic film with fs pulse. They found that sub-spot size feature can be obtained by the precise control of the peak fluence just above the threshold fluence. When the peak fluence is 2% higher than threshold value we can get a feature size of one-tenth the size of laser spot. Authors fabricated holes of diameter less than 200 nm with focused laser spot of 1.7 mm in 100 mm thick metallic thin film. Dausinger 2003-[9] found that fs lasers have certain disadvantages like deformation of laser beam near the focus and deflection of s-polarized radiation at hole wall. No significant change in thermal behavior is observed when the pulse duration is below 10 ps whereas the scattering effect increases when pulse width is less than 5 ps, therefore pulse duration of 5–10 ps is more suitable for micromachining of metals. Rizvi 2003-[10] reviewed the applicability of fs laser for micromachining of different types of materials. It was found that the waveguide writing is the only unique application where no other laser except fs can be applied. It was observed that ns laser pulses could also produce similar results for certain materials. Kamlage et al. 2003-[11] have demonstrated that the fs laser is suitable to fabricate microholes with special geometries, superior quality and high reproducibility. Tong et al. 2004-[12] have explored the prospect of fabricating embedded microheater patterns in thermal sprayed nichrome alloy coatings on alumina substrates. . Heater patterns have been designed to produce a uniform heat flux, a linear distributed heat flux and a non-uniform heat flux for uniform temperature distribution.

2. Experimental set up

The experiments, set up to study the influence of the process parameters, were carried out through 30 watt Fiber Laser (air cooled, digitally controlled, co2 laser tubes are fully modular and permanently aligned and field replaceable) with pulsed 20-80 kHZ and resolution user controlled choice of 75, 150, 200, 300, 400, 600 or 1200 dpi. The sample of material was stainless steel, selected because it is a widely used material in various industries. Dimensional measurements were performed with digital microscope (Dinolite 2) and 3D optical profilometer Contour GT (Bruker).

Several micro-channels were machined in each case changing one single parameter while the other remained fixed. By this, we could see the effect of single control variable, in order to determine the control parameter range. Variable factors and factor levels presented in Table 1, which is used to study effect of the input. Micro-channels array (20 x 20) has been fabricated in a 10 mm x 10 mm x 1.3 mm rectangular stainless steel plates. In the experiments influence of process parameters such as scanning speed (SS), pulse intensity (PI) and pulse frequency (PF) were carried out with Epilog Laser Fiber Mark Fusion Machine model -13000.

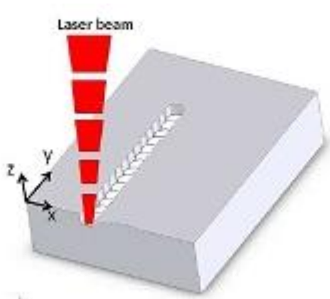

Fig 1: A schematic illustration of the Fiber Laser machining.

Table 1. Variable factors and factor levels.

Variable Factors	Factor Levels			
Scanning Speed (SS) in %	30	50	70	90
Pulse Intensity (PI) in %	50	70	90	-
Pulse Frequency (PF) in %	30	50	70	90

3. Experimental results and discussion

48 samples were machined with the laser machining process by following the design of experiments as summarized in Table 1. Dimensional measurement for each micro-channel, take three different locations on same sample and evaluate average these measurements for depth and width of micro-channels. 48 micro-channels were machined and experimental results were obtained, these machined features for all the combinations of the variable factors are shown in Table 2. The micro-channels have variations in dimensions and shape. These variations in micro-channels are clearly shown in Figure 2, 3 and 4. Analysis of variance was performed for each response factor to understand the influence of the process parameters. It is evident from figure 2 that the width of the channel decreases and depth increases as PI increases. The images in figure 3 indicate that as SS increases the depth increases and width decreases.

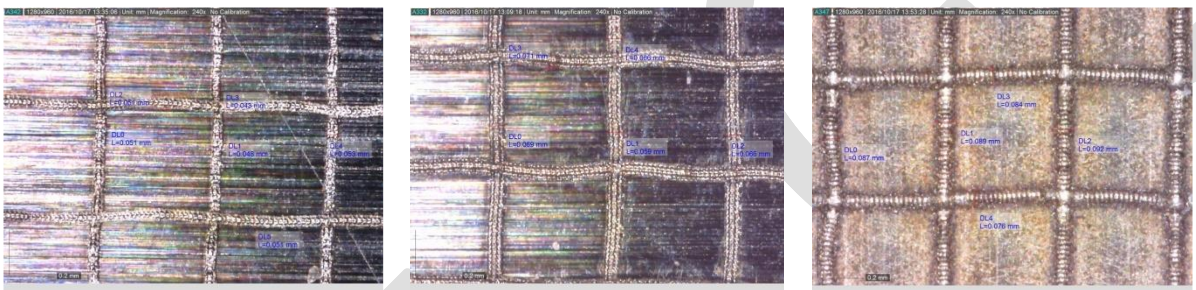

(a) (b) (c)

Fig 2: Images of micro-channels for Pulse Intensity (a) 50% (b) 70% and (c) 90%, for constant Scanning Speed 70%, and Pulse Frequency 30% taken from Digital Microscope.

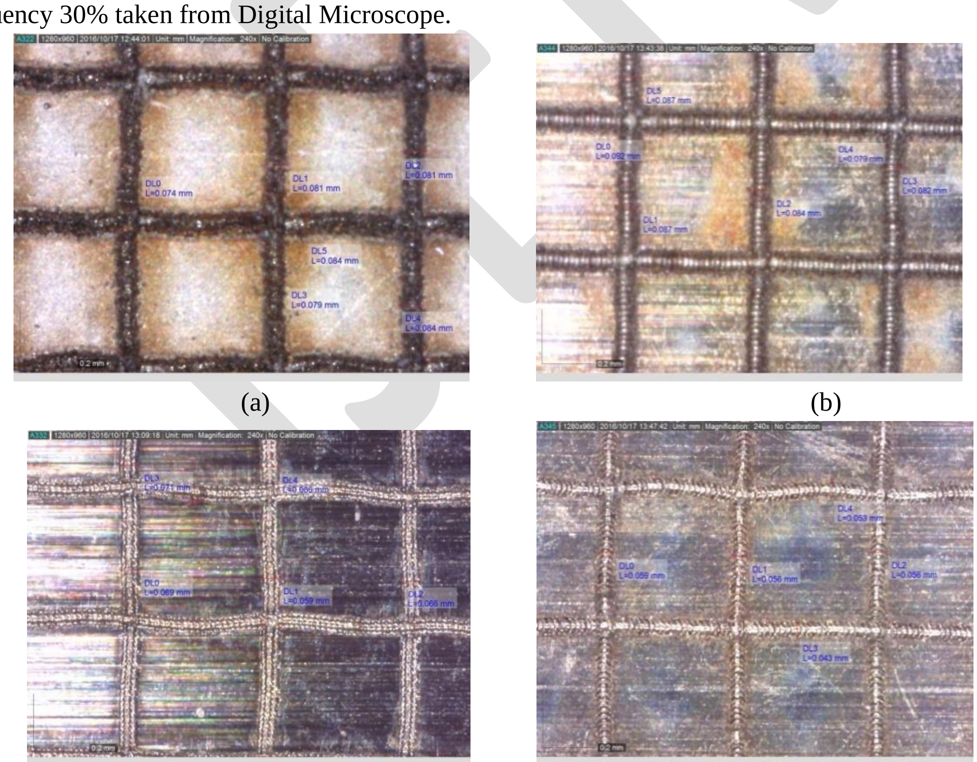

(a) (b)

(c) (d)

International Journal of Engineering Research and General Science Volume 5, Issue 6, November-December, 2017
ISSN 2091-2730

Fig 3: Images of micro-channels for Scanning Speed (a) 30% (b) 50%, (c) 70%, and (d) 90% for constant Pulse Intensity 70%, and Pulse Frequency 30% taken from Digital Microscope.

The images taken from 3-D Profilometer as shown in fig 4 indicates that as the PF increases the visibility of microchannels are poor.

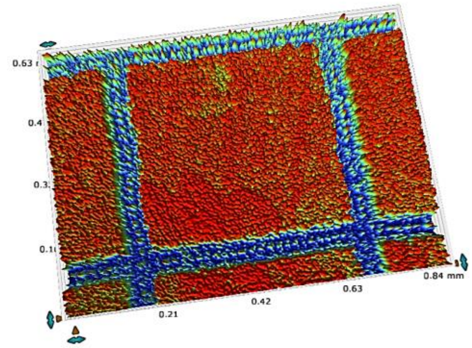

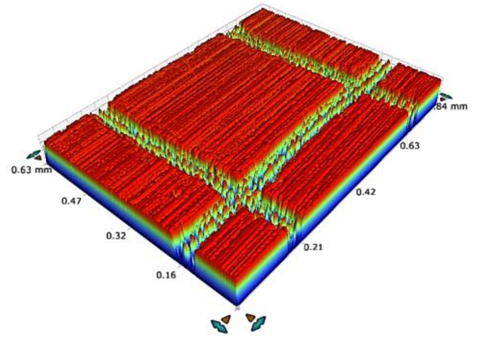

(a) **(b)**

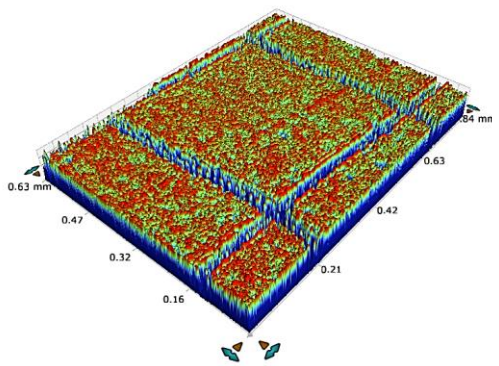

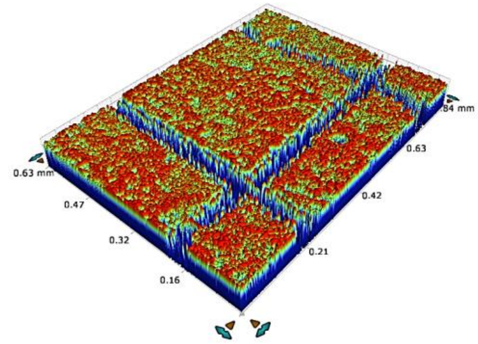

(c) (d)

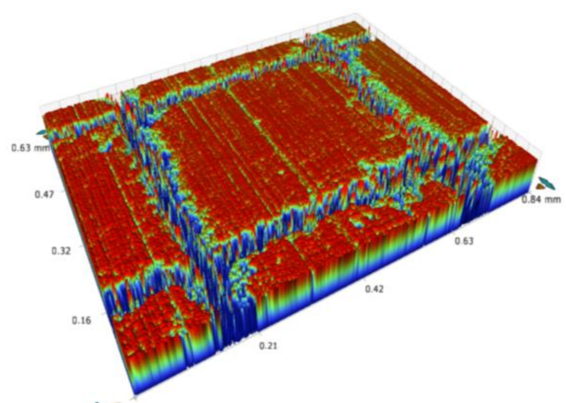

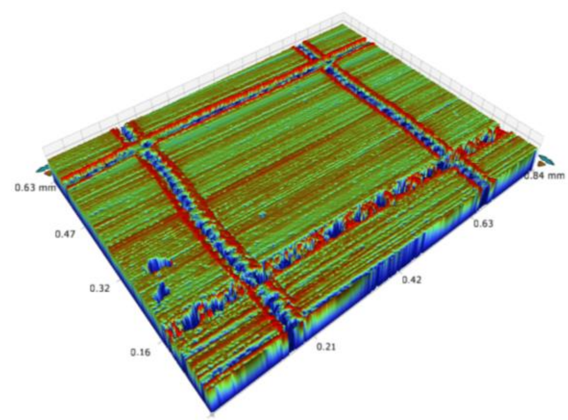

] P]

70%, PI 70% and PF 70% and (d) SS 90%, PI 90% and PF 90%, (e) SS 30,PI 30,PF 30 (f) SS30,PI 90,PF 90

Table 2 Experimental results with Input control variables

				Digital Micrometer	3D Optical Profilometer
SL No	SS %	PI %	PF %	Width (μm)	Depth (μm)
1	30	50	30	35	7.402
2	50	50	30	30	7.054
3	70	50	30	38	6.675
4	90	50	30	28	3.867
5	30	70	30	60	8.860
6	50	70	30	60	7.860
7	70	70	30	43	7.780
8	90	70	30	43	7.213
9	30	90	30	65	9.894
10	50	90	30	72	8.832
11	70	90	30	62	8.325
12	90	90	30	60	7.901
13	30	50	50	41	7.330
14	50	50	50	37	7.810
15	70	50	50	26	5.190
16	90	50	50	37	3.712
17	30	70	50	53	8.901
18	50	70	50	58	7.120
19	70	70	50	57	8.321
20	90	70	50	50	5.013
21	30	90	50	63	11.980
22	50	90	50	56	11.690
23	70	90	50	57	10.580
24	90	90	50	60	9.865
25	30	50	70	38	6.432
26	50	50	70	39	4.010
27	70	50	70	45	3.450
28	90	50	70	34	3.123
29	30	70	70	48	7.320
30	50	70	70	48	6.890
31	70	70	70	51	5.560
32	90	70	70	42	5.345
33	30	90	70	70	9.986
34	50	90	70	58	9.894
35	70	90	70	57	8.523
36	90	90	70	57	7.860
37	30	50	90	31	7.356
38	50	50	90	34	7.032
39	70	50	90	20	6.867
40	90	50	90	18	5.899

41	30	70	90	56	8.245
42	50	70	90	45	9.420
43	70	70	90	48	7.986
44	90	70	90	49	6.896
45	30	90	90	66	11.045
46	50	90	90	58	10.891
47	70	90	90	56	10.590
48	90	90	90	53	9.874

3.1 Micro-channel depth

With the help of Table 2's results obtained for micro-channel depths, the influence of the scanning speed and the pulse intensity on the depth dimensions is summarized in figure 5.

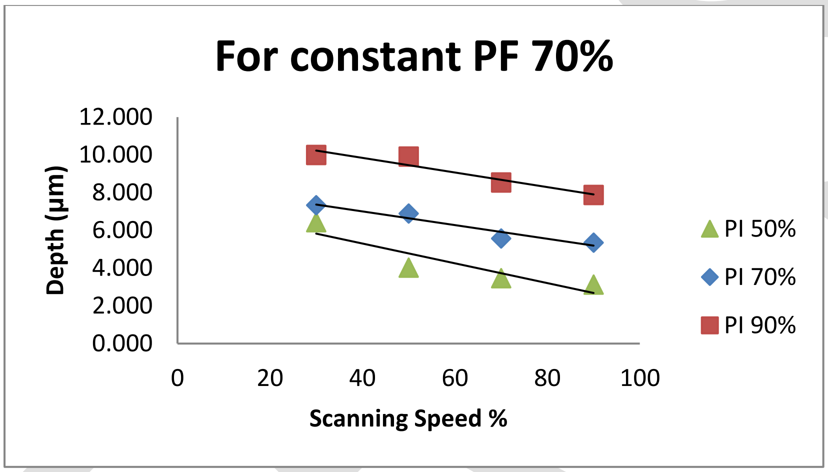

Fig 5: Influence of scanning speed and pulse intensity on depth dimension

The trend lines in figure 5 shows that higher scanning speeds produce smaller depths and higher pulse intensities produce in deeper micro-channels. Higher pulse intensities and lower scanning speeds result in deeper micro-channels because the surface is machined with high energy for longer time, which allows a large amount of energy to be absorbed by the work-piece. So figure 4 explains that for higher depths, higher pulse intensity values would be necessary.

Table summarizes the result of the ANOVA revealing that the significant factors for the average depth of micro- channels are pulse intensity and scanning speed.($p<0.05$). The F value indicates that the pulse intensity is the most significant factor, which is made clear by the contribution value.

Table 3: ANOVA Result for 3 D optical profilometer depth

Source	Sum of Squares	DOF	Mean Square	F Value	P Value	Contribution (%)
A-SS	*36.2*	*1*	*36.2*	*28.81*	*0.0001*	21.688335
B-PI	*130.09*	*1*	*130.09*	*103.55*	*0.0001*	77.9402073
C-PF	*0.62*	*1*	*0.62*	*0.49*	*0.4862*	0.37145767
Residual	55.28	44	1.26			
Cor Total	222.19	47				

3.2 Micro-channel width

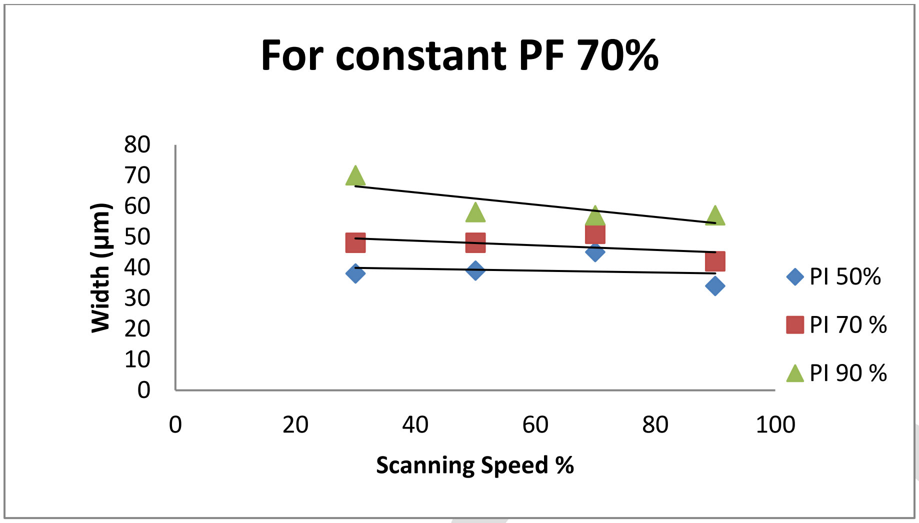

Fig6: Influence of scanning speed and pulse intensity on width dimension

The table 2 presents width dimension that range from 18 to 72 µm. Figure 6 shows how the scanning speed and the pulse intensity affect the width. The trend lines in figure 6 shows that higher scanning speeds produce smaller width. Thus, as the channel becomes deeper, the width becomes greater.

Source	Sum of Squares	DOF	Mean Square	F Value	P Value	Contribution (%)
A-SS	*426.67*	*1*	*426.67*	*13.8*	*0.0006*	6.45880576
B-PI	*6022.53*	*1*	*6022.53*	*194.75*	*0.0001*	91.1672989
C-PF	*156.82*	*1*	*156.82*	*5.07*	*0.0294*	2.37389533
Residual	1360.65	44	30.92			
Cor Total	7966.67	47				

Table 4: ANOVA Result for width

The table 4 summarizes the result of the ANOVA revealing that all the factor (Scanning speed, pulse intensity and pulse frequency) have significant influence on the width ($p<0.05$) in contrast to Teixidor, Grzenda et al [1]. The experimental results shows that the significant importance of pulse frequency. The F value indicates that the pulse intensity is the most significant factor followed by scanning speed and pulse frequency.

Conclusion

The study reveals that Fibre-laser machining process is suitable for fabricating micro-channels. In this study, dimensional features and the productivity of micro-channels have been studied. Although the results obtained for the micro-channels present variations, they do suggest that laser machining is capable of producing micro-geometries. Several specific conclusions should be pointed out:

1. Low scanning speeds and high pulse intensities increase the depth and decrease the width of the micro-channels.
2. The surface quality of the channels improves with a rise in scanning speed, and surface quality improves with at lower Pulse Frequency.
3. Laser micromachining productivity increases with high pulse intensities and low scanning speeds.
4. ANOVA results show that PF is also statistically significant along with PI and SS for the responses under study of width of micro channel.
5. ANOVA results show that PF is statistically insignificant for the responses under study of depth of micro channel.

Future work will consider other AI techniques for validation of study, such as ensembles of classifiers or regressors. These ensembles are built by combining different basic classifiers that could improve final model accuracy. Non-linear models will also be tested, such as non-linear regressors, to ensure that any interaction effect is taken into account and evaluated.
Further, the rate of heat transfer can also be studies and modelled for better understanding the response of micro-channels under various parameters.

REFERENCES:

1. Teixidor, D., Grzenda M., Bustillo, A., Ciurana, J., "Modelling pulsed laser micro-machining of micro-geometries using machine-learning techniques", Journal of Intelligence Manufacturing, june 2013.

2 .E. V. Bordatchev and S. K. Nikumb, "An Experimental Study and Statistical Analysis of the Effect of Laser Pulse Energy on the Geometric Quality During Laser Precision Machining", MACHINING SCIENCE AND TECHNOLOGY Vol. 7, No. 1, pp. 83–104, 2003.

3. Basem. F. Yousefa, George K. Knopfa, Evgueni V. Bordatchevb, Suwas K.Nikumb, "Neural network modeling of the laser material-removal process", Sensors and Controls for Intelligent Manufacturing II, Peter E. Orban, Editor, Proceedings of SPIE Vol. 4563 (2001).

4. Kant Rishi, Gupta Ankur, Bhattacharya S., "Studies on CO2 laser micromachining on PMMA to fabricate micro channel for microfluidic applications", 5th International & 26th All India Manufacturing Technology, Design and Research Conference (AIMTDR 2014) December 12th–14th, 2014, IIT Guwahati, Assam, India.

5. Semaltianos NG, Perrie W, "Picosecond laser ablation of nickel-based superalloy C263", Applied physics A; Materials Science and Processing Vol 98(2), pp.345-355 (2010).

6. Cadot G.B.J , Axinte D.A. ,.Billingham J, "Continuous trench, pulsed laser ablation for micro-machining applications" International Journal of Machine Tools & Manufacture 107, pp.8-20 (2016).

7. Venkatakrishnan K, Tan B, Ngoi BKA. Femtosecond pulsed laser ablation of thin gold film. Opt Laser Technol ;34 pp.199–202 (2002).

8. Venkatakrishnan K, Tan B, Sivakumar NR. Sub-micron ablation of metallic thin film by femtosecond pulse laser. Opt Laser Technol;34, pp575 (2002).

9. Dausinger F. Femtosecond technology for precision manufacturing: fundamental and technical aspects. RIKEN Rev;50: pp77–82, (2003).

10. Rizvi NH. Femtosecond laser micromachining: current status and applications. RIKEN Rev 50:pp77-82 (2003).

11. Kamlage G, Bauer T, Ostendorf A, Chichkov BN. Deep drilling of metals by femtosecond laser pulses. Appl Phys A;77 pp.307 , (2003).

12. Tong T, Li J, Chen Q, Longtin JP, Tankiewicz S, Sampath S. Ultrafast laser micromachining of thermal sprayed coatings for microheaters: design, fabrication and characterization. Sens Actuator A;pp.114:102 (2004).

STUDIES ON INFLUENCE OF INJECTION PRESSURE ON EXHAUST EMISSIONS OF DIESEL ENGINE WITH MEDIUM GRADE INSULATED COMBUSTION CHAMBER WITH CRUDE JATROPHA OIL OPERATION

Dr.N. Janardhan
[1,]Mechanical Engineering Department, Chaitanya Bharathi Institute of Technology,
Gandipet, Hyderabad 500075, Telangana State, India,
[1]E-mail: narambhatlu.datta@gmail.com

Abstract–In the context of depletion of fossil fuels, evar increase of pollution levels with fossil fuels, search for alternative fuels has become pertinent. Vegetable oils are important substitutes for diesel fuel as their properties are comparable to diesel fuel. Investigations were carried out to study exhaust emissions of diesel engine with air gap insulated low heat rejection (LHR–2) combustion chamber consisting of air gap insulated piston with 3 mm air gap, with superni (an alloy of nickel) crown and air gap insulated liner with superni insert with varied injector opening pressure. Exahsut emissions [particulate emissions and nitrogen oxide levels] were determined at various values of brake mean effective pressure (BMEP) of the LHR–2 combustion chamber and compared with neat diesel operation on conventional engine (CE) and vegetable oil operation at similar operating conditions. Engine with LHR–2combustion chamber with vegetable oil operation showed reduction of particulate emissions at manufacturer's recommended injection timing of 27^{o} bTDC, and these emissions decrased marginally with increased injector opening pressure n comparison with CE with diesel and vegetable oil at 27^{o}bTDC. However, LHR-2 engine drastically increased nitrogen oxide levels in comparion with conventional engine with vegetable oil.

Index Terms– Alternative fuels, Vegetable oil, Exhasut emissions, Particulate Emissions, Nitrogen oxide levels, Conventional engine, LHR engine, Injection pressure.

1.INTRODUCITON

Non-edible vegetable oils can be seriously considered as alternative fuels for engines as their properties are comparable to diesel fuels and also edible oils are in great demand and are far too expensive as fuels. When Rudolph Diesel, first invented the diesel engine, about a century ago, he demonstrated the principle by employing peanut oil and hinted that vegetable oil would be the future fuel in the diesel engine [1]. Several researchers experimented the use of vegetable oils as fuel on conventional engines (CE) and reported that the performance was poor, citing the problems of high viscosity, low volatility and their polyunsaturated character causing the problems of piston ring sticking, injector and combustion chamber deposits, fuel system deposits, reduced power, reduced fuel economy and increased exhaust emissions [1]–[8]. The presence of the fatty acid components greatly affects the viscosity of the oil, which in turn affect the wear of engine components, oil consumption, fuel economy, hot starting, cold starting, low temperature pumpability, noise and shear stability. The limitation of unsaturated fatty acids is necessary due to the fact heating higher unsaturated fatty acids results in polymerization of glycerides. This can leads to formation of deposits or to deterioration of lubricating oil. The different fatty acids present in the vegetable oil are palmic, steric, lingoceric, oleic, linoleic and fatty acids [1]. These fatty acids increase particulate emissions and also lead to incomplete combustion due to improper air–fuel mixing. Studies were made with single cylinder, four-stroke water cooled direct injection diesel engine, with 3.68 kW brake power at a speed of 1500 rpm with a compression ratio of 16:1 with vegetable oils with varied injector opening pressure and injection timing.[5]-[6]. The injection timing was varied by inserting copper shims in between pump body and engine frame, while change of injector opening pressure was achieved by using nozzle–testing device. At manufacturer's recommended injection timing of 27^{o} bTDC, particulate emissions increased by 56%, while nitrogen oxide (NO_x) levels decreased by 18% with crude vegetable oil when compared with neat diesel operation on conventional engine. Particulate emissions decreased by 15–20%, while NO_x levels increased by 15–20% with conventional engine with crude vegetable oil operation with an increase of injector opening pressure of 80 bar, when compared with neat diesel operation.

Experiments were conducted on preheated vegetable oil in order to equalize their viscosity to that of pure diesel may ease the problems of injection process [5]–[6]. Investigations were carried out on conventional four stroke diesel engine, 3.68 kW at a speed of 1500 rpm with preheated vegetable oil with varied injection timing and injection pressure. They reported that preheated vegetable oil at 27^{o} bTDC, decreased particulate matter emissions by 8–9%, NO_x emissions by 5–6%, when compared with normal vegetable oil.

Increased injector opening pressure may also result in efficient combustion in compression ignition engine It has a significance effect on the performance and formation of pollutants inside the direct injection diesel engine combustion. Experiments were conducted on conventional four stroke diesel engine, with neat diesel operation with increased injector opening pressure. [9]–13]. They reported that particulate emissions decreasd while NO_x levels increased with an increase of injection pressure.

Experiments were conducted on conventional four stroke diesel engine, 3.68 kW at a speed of 1500 rpm with vegetable oil operation with increased injector opening pressure. They reported that performance of the engine improved with increased injector opening pressure with vegetable oil operation.[5]–[6]. It decreased particulate emissions by 20–22% and increased NO_x levels by 10–14% with an increase of injector opening pressure by 80 bar.

The drawbacks associated with biodiesel (high viscosity and low volatility) call for hot combustion chamber, provided by low heat rejection (LHR) combustion chamber. The concept of the engine with LHR combustion chamber is reduce heat loss to the coolant, by providing thermal resistance in the path of heat flow to the coolant. Any saving in this part of the energy distribution would either increase the energy lost through exhaust gases or increase the power output. Considerable efforts are under way to reduce heat loss to the coolant by various researchers. However, the results are a little confusing as to whether the insulation would improve or deteriorate thermal efficiency. Three approaches that are being pursued to decrease heat rejection are (1) Coating (low grade LHR combustion chamber) with low thermal conductivity materials on crown of the piston, inner portion of the liner and cylinder head, (2) air gap insulation (medium grade LHR combustion chamber) where air gap is provided in the piston and other components with low-thermal conductivity materials like superni, cast iron and mild steel and (3).Combination of low grade and medium grade LHR combustion chambers results in high grade LHR combustion chamber.

Experiments were conducted on high grade LHR combustion chamber, consisting of air gap (3 mm) insulated piston with superni crown, fitted to the body of the piston by threading by keeping a gasket made of superni material, air gap insulated liner with superni insert and ceramic coated cylinder head (partially stabilized zirconium of thickness 500 microns coated on inside portion of cylinder head) with vegetable oil with varied injector opening pressure and injection timing [14]-[17]. They reported from their investigations, that thermal efficiency increased by 3-41%, volumetric efficiency increased by 2-3%, particulate emissions decreased by 20-25% NOx levels decreased by 20-25%, peak pressure increased by 20-25% and maximum rate of pressure increased by 6-8% with engine with LHR combustion chamber with vegetable oil operation with an increase of injector opening pressure of 80 bar when compared with neat diesel operation on conventional engine at 27^o bTDC.

Little reports were avialble on comparative studies of exahsut emissions of medium grade LHR engine with crude jatropha oil and diesel with varied injector opening pressure and at different operating condtions of the vegetable oil. The authors have made an attempt in this direction. Studies were made on exaust emissions of medium grade LHR engine consisted of air gap insulated piston and air gap insulated liner with different operating condtions of the crude vegetable oil with varied injector opening pressure and compared with vegetable oil with convetniona engine.

2.MATERIALS AND METHODS

2.1 Crude Vegetable Oil

India with just 2.4% of the global area supports more than 16% of world's human population and 17% of the cattle population. According to economic survey (2000-2001), of the cultivable land area, about 175 million hectares are classified as waste and degraded or marginal land. If the non forest waste-lands could be used to cultivate plants which can survive on such soil and which can produce oilseeds, these could be effectively used to combat fuels shortage in the country and at the same time bring such degrade lands back to its productive capacity.

Jatropha (Jatropha curcas, Ratanjyot) is a suitable candidate for its purpose. Jatropha oil [18] known as moglaerand, beghierand, chandsaiyoti, or nepalam in Inida can be substituted for diesel. India imports jatropha oil of worth about 400 crores annually, which is used for making soap. Jatropha is a large shrub or small tree found throughout the tropical and subtropical regions of the world. The plant has several distinguishing and useful properties such as hardness, rapid growth easily propagation and wide ranging usefulness. It grows on any type of soil and is well adapted to cultivation. The plant has no major diseases or insect pests and is not browsed by cattle or sheep even during times of drought. The plant can survive for more than a year without water. Propagation is easily achieved by seed or stem cutting and its growth is rapid as is implied by its ability to form a thick live hedge nine months after planting. The plant starts yielding form the third year onwards and continues to yield for the next 25 years. The whole seeds can be crushed to yield about 25%oil. Double crushing can increase the yield to 28.5%and solvent extraction to 30%. The yield from established plantations in Brazil is around 1.5 to 2.3 tons per hectare. The seed and oil possess toxins and hence non-edible. The oil cake is also toxic and can be used only as manure and is very useful for this application with high nitrogen content and a favorable N: P: K ratio of 2.7:1.2:1. The properties of vegetable oil are shown in Table.1

TABLE.1

PROPERTIES OF TEST FUELS

Test Fuel	Viscosity at 25^oC (centi-poise)	Specific gravity at 25^o C	Cetane number	Lower Calorific value (kJ/kg)
Diesel	12.5	0.84	55	42000
Jatropha oil (crude)	125	0.90	45	36000

International Journal of Engineering Research and General Science Volume 5, Issue 6, November-December, 2017
ISSN 2091-2730

ASTM Standard	ASTM D 445	ASTM D 4809	ASTM D 613	ASTM D 7314

2.2 Engine With LHR Combustion Chamber

Engine with high grade LHR combustion chamber contained a two–part piston. (Fig.1) the top crown made of low thermal conductivity material, superni was screwed to aluminum body of the piston, providing a 3mm air gap in between the crown and the body of the piston. The optimum thickness of air gap in the air gap piston was found to be 3 mm for improved performance of the engine with superni inserts with diesel as fuel [19]. A superni insert was screwed to the top portion of the liner in such a manner that an air gap of 3mm was maintained between the insert and the liner body. At 500 ºC the thermal conductivity of superni and air are 20.92 and 0.057 W/m–K. The combination of low thermal conductivity materials of air and superni provide sufficient insulation for heat flow thus resulting LHR combustion chamber.

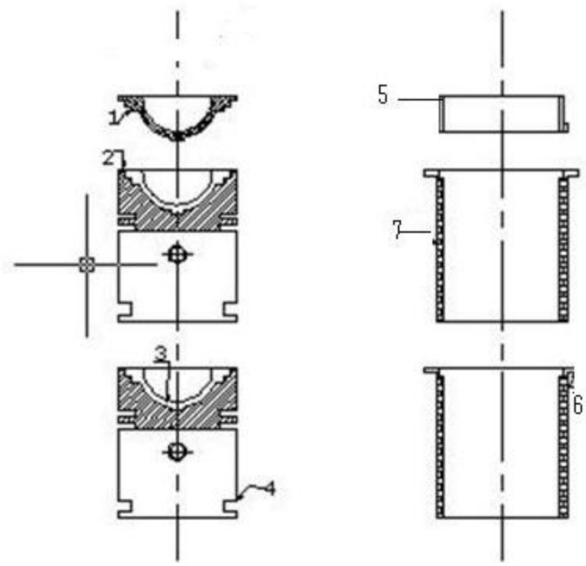

1.Superni piston crown with threads, 2. Superni gasket, 3. Air gap in piston, 4. Body of piston, 5.Superni insert with threads, 6.Air gap in liner, 7.Liner

Fig.1 Assembly details of air gap insulated piston, air gap insulated liner and ceramic coated cylinder head

2.3 Experimental Set–Up

The schematic diagram of the experimental setup used for the investigations on the engine with LHR combustion chamber with cotton seed oil based biodiesel is shown in Fig.2. Specifications of the test engine were given in Table 2. The engine tests were carried out with a single–cylinder, four–stroke, naturally aspirated, compression ignition engine with brake power 3.68 k W at a speed of 1500 rpm. The compression ratio of engine was 16:1. Manufacturer's recommended injection timing and injector opening pressure were 27º bTDC and 190 bar. The engine was connected to an electric dynamometer for measuring its brake power. Dynamometer was loaded by a loading rheostat. The accuracy of engine load was ±0.2 kW. The speed of the engine was measured with digital tachometer with accuracy ±1%. The fuel consumption was registered with the aid of fuel measuring device (Burette and stop watch). The accuracy of brake thermal efficiency obtained is ±2%. Vegetabe oil was injected into the engine through conventional injection system. Provision was made for preheating of vegetable oil to the required levels (90ºC) so that its viscosity was equalized to that of diesel fuel at room temperature.

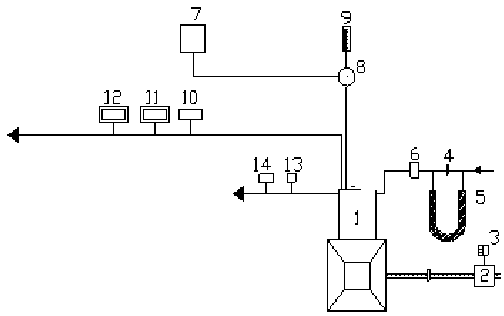

1.Engine, 2.Electical Dynamo meter, 3.Load Box, 4.Orifice meter, 5.U-tube water manometer, 6.Air box, 7.Fuel tank, 8, Three way valve, 9.Burette, 10. Exhaust gas temperature indicator, 11.AVL Smoke meter, 12.Netel Chromatograph NOx Analyzer, 13.Outlet jacket water temperature indicator and 14. Outlet-jacket water flow meter.

Fig.2. Schematic diagram of experimental set–up

Air-consumption of the engine was obtained with an aid of air box, orifice flow meter and U–tube water manometer assembly. Air–box with diaphragm was used to damp out the pulsations produced by the engine, for ensuring a steady flow of air through the intake manifold. The naturally aspirated engine was provided with water-cooling system in which outlet temperature of water was maintained at 80ºC by adjusting the water flow rate. The water flow rate was measured by means of analogue water flow meter, with accuracy of measurement of ±1%.

TABLE.2.
SPECIFICATIONS OF THE TEST ENGINE

Description	Specification
Engine make and model	Kirloskar (India) AV1
Maximum power output at a speed of 1500 rpm	3.68 kW
Number of cylinders ×cylinder position× stroke	One × Vertical position × four-stroke
Bore × stroke	80 mm × 110 mm
Method of cooling	Water cooled
Rated speed (constant)	1500 rpm
Fuel injection system	In-line and direct injection
Compression ratio	16:1
BMEP @ 1500 rpm	5.31 bar
Manufacturer's recommended injection timing and pressure	27ºbTDC × 190 bar
Dynamometer	Electrical dynamometer
Number of holes of injector and size	Three × 0.25 mm

Engine oil was provided with a pressure feed system. No temperature control was incorporated, for measuring the lube oil temperature. Change of injector opening pressure from 190 bar to 270 bar (in steps of 40 bar) was made using nozzle testing device. The maximum injector opening pressure was restricted to 270 bar due to practical difficulties involved. Coolant water jacket inlet temperature, outlet water jacket temperature and exhaust gas temperature were measured by employing iron and iron-constantan thermocouples connected to analogue temperature indicators. The accuracies of analogue temperature indicators are ±1%. Particulate emissions were measured by AVL Smokemeter, while nitrogen oxide (NO_x) levels were determined by Netel Chromatograph NO_x Aanlyzer at various values of brake mean effective pressore (BMEP) of the engine. The measuring principle and repeatability of these analyzers was given in Table.3. Analyzers were allowed to adjust their zero point before each measurement. To ensure that accuracy of measured values was high, the gas analyzers were calibrated before each measurement using reference gases.

TABLE.3

SPECIFICATIONS OF THE

SMOKE OPACIMETER (AVL, INDIA, 437). AND NO_X ANALYZER (NETEL INDIA, (4000 VM))

Pollutant	Measuring Principle	Range	Least Count	Repeatability
Particulate Emissions	Light extinction	1–100%	0.1% of Full Scale (FS)	0.1% for 30 minutes
NO_x	Chemiluminiscence	1–5000 ppm	0.5% of FS	≤0.5% F.S

3.RESULTS AND DISCUSSION

Various exhaust emissions measured were particulate emissions and nitrogen oxide levels at various values of brake mean effective pressure of the engine

Fig.3 shows variation of particulate emissions with brake mean effective pressure in conventional engine and LHR-2 engine at at 27^o b TDC and injector opening pressure of 190 bar.,with crude jatropha oil operation. Similar characteristics with neat diesel operation on conventional engine at recommended injection timing was also shown for comparison purpose.

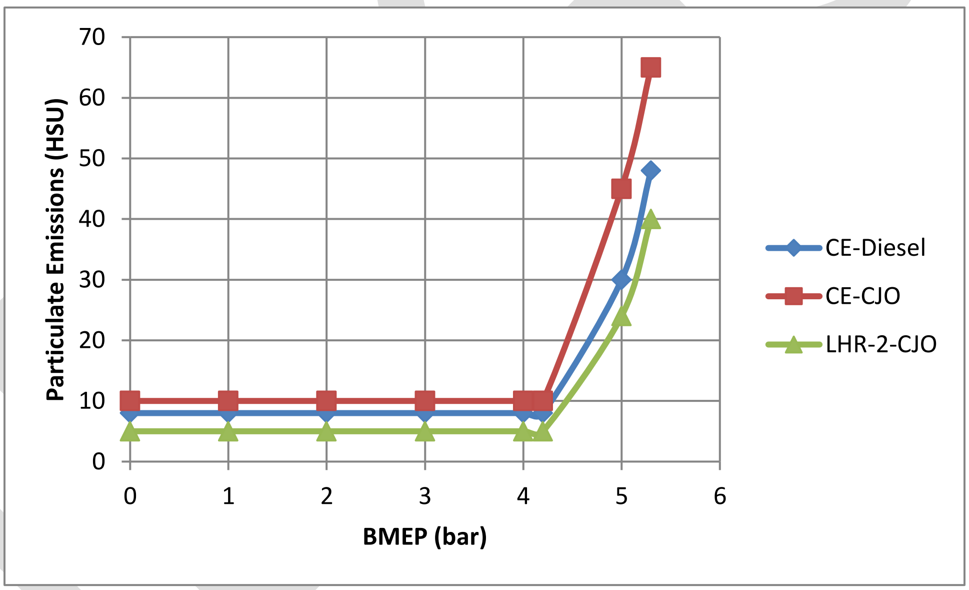

Fig.3 Variation of particulate emissions with brake mean effective pressure (BMEP) in conventional engine (CE) and LHR-2engine with crude jatropha oil (CJO) operation at 27^o b TDC and injector opening pressure of 190 bar.

Particulate emissions were more or less constant during part load and suddenly at 80% of the full load, they increased with both versions of the combustion chamber. This was due to excess air fuel ratios at part load and decrease of the same at full load. Conventional engine with crude vegetable oil showed the deterioration in the performance at all loads when compared with the neat diesel operation on conventional engine at recommended injection timing. From this Fig, it is observed that drastic increase of particulate emissions at all loads with vegetable oil operation was observed compared with neat diesel operation. This was due to the higher value of ratio of C/H (0.7 for vegetable oil while it is 0.45 for diesel) in fuel composition. (C= Number of carbon atoms and H= Number of hydrogen atoms in fuel composition ($C_{18}H_{27}O_6$). Higher the value of this ratio means, number of carbon atoms is higher, leading to produce higher levels of carbon dioxide and carbon monoxide and hence higher particulate emissions. The increase of particulate emissions was also due to reduction of oxygen-fuel ratios and volumetric efficiency with vegetable oil operation. Different fatty acids present in the crude vegetable oil are palmic, steric,

lingoceric, oleic, linoleic and fatty acids [5]. These fatty acids increase particulate emissions and also lead to incomplete combustion due to improper air-fuel mixing.

This was also because of higher viscosity of vegetable oil. Particulate emissions are related to the density of the fuel. Since crude vegetable oil has higher density compared to diesel fuel, particulate emissions were higher with vegetable oil. Particulate emissions at all loads decreased at the optimum injection timing with vegetable oil operation with both versions of the combustion chamber. This was due to early initiation of combustion with increased contact of fuel with air leading to improve atomization.

Fig.4. presents bar charts showing the variation of particulate emissions at full load operation with test fuels at recommended at an injector opening pressure of 190 bar. Conventional engine increased particulate emissions at full load by 35% at 27^o bTDC when compared with neat diesel operation. This was due to fuel composition, higher density and deteriorated of combustion of vegetable oil with conventional engine. LHR-2 engine with vegetable oil reduced particulate emissions by 42% at 27^o bTDC in comparison with diesel operation on same configuration of the engine. This showed that combustion improved with hot environment and higher heat release rate with LHR-2 engine with vegetable oil operation in comparison with diesel operation.
LHR-2 engine with vegetable oil operation reduced particulate emissions at full load by 46% at recommended injection timing in comparison with conventional engine with vegetable oil operation. This was due to reduction of ignition delay with higher duration of combustion of vegetable oil with which improved combustion leading to reduce particulate emissions. Reduction of ignition delay of higher cetane value of diesel fuel leads to fuel cracking and hence higher particulate emissions with LHR-2 engine with diesel as fuel. Thus once again, it is confirmed that LHR-2 engine was more suitable for vegetable oil operation.

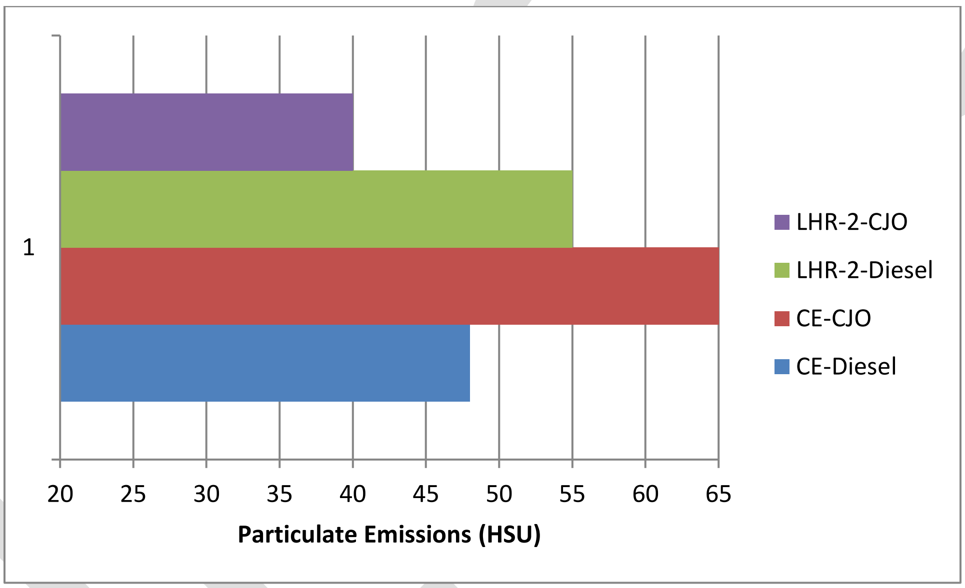

Fig. 4. Bar charts showing the variation of particulate emissions at full load operation with conventional engine and LHR-2 engine with neat diesel and crude jatropha oil operation.

LHR-2 engine with vegetable oil operation reduced particulate emissions at full load by 27% at recommended injection timing when compared with neat diesel operation on conventional engine. This showed that combustion improved with LHR-2 engine with vegetable oil operation. Particulate emissions at full load were observed to be higher with conventional engine with vegetable oil at recommended injection timing.
Nitrogen oxide (NO_x) levels are the precursor pollutants which can combine to form photochemical smog. These irritate the eyes and throat, reduces the ability of blood to carry oxygen to the brain and can cause headaches, and pass deep into the lungs causing respiratory problems for the human beings. Long-term exposure has been linked with leukemia. Therefore, the major challenge for the existing and future diesel engines is meeting the very tough emission targets at affordable cost, while improving fuel economy.
Temperature and availability of oxygen are two favorable conditions to form NOx levels. Fig. 5. shows the variation of nitrogen oxide levels with brake mean effective pressure with both versions of the combustion chamber at recommended and injection timing with vegetable oil operation at an injector opening pressure of 190 bar. NO_x levels increased with increase of brake mean effective pressure with vegetable oil operation at recommended and optimized injection timing due to higher peak pressures, temperatures as larger regions of gas burned at close-to-stoichiometric ratios particularly at full load operation. Conventional engine registered lower at all loads with vegetable oil operation when compared with diesel operation. This was due to deterioration of combustion due its high viscosity, low volatility and low calorific value of the fuel of the vegetable oil at recommended injection timing leading to produce low temperatures and hence lower NOx levels.

Drastically increase of NO_x emissions were observed at all loads with engine with LHR-2 combustion chamber with vegetable oil operation when compared with neat diesel operation on conventional engine. This was because of increase of peak pressures and temperatures due to reduction of ignition delay with hot environment provided by the engine with LHR-2 version of the combustion chamber.

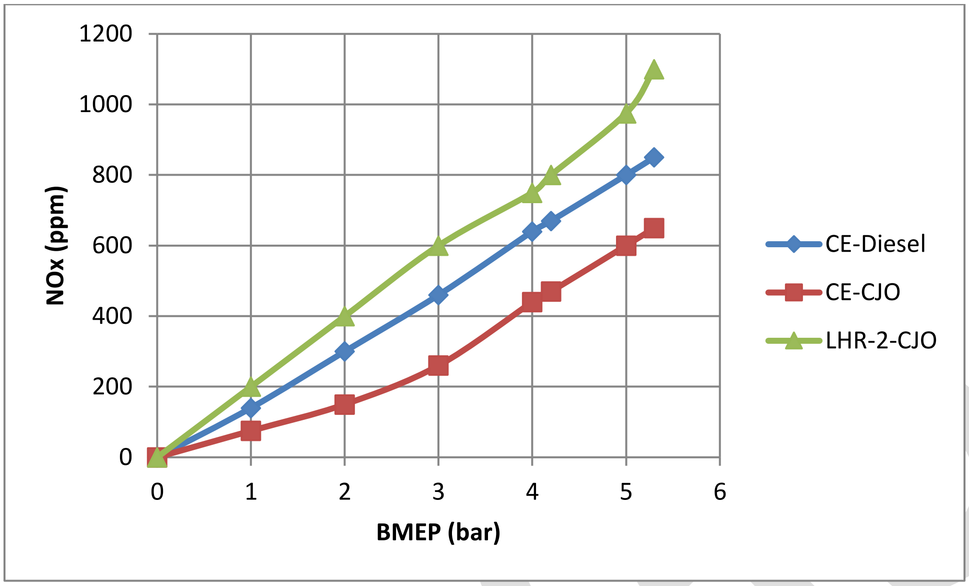

Fig.5. Variation of nitrogen oxide levels (NOx) with brake mean effective pressure (BMEP) with conventional engine and LHR-2 engine with crude vegetable oil operation at recommended injection timing at an injector opening pressure of 190 bar.

Fig.6. presents bar charts showing the variation of particulate emissions at full load operation with test fuels at recommended injection timing at an injector opening pressure of 190 bar.

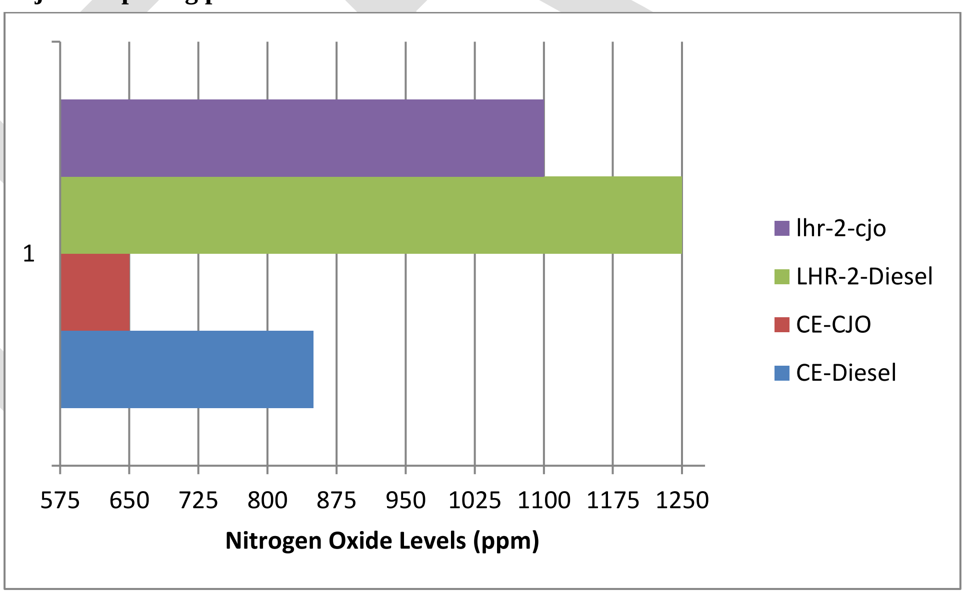

Fig.6. Bar charts showing the variation of nitrogen oxide levels (NO_x) at full load operation with conventional engine and LHR-2engine with neat diesel and crude jatropha oil operation.

Conventional engine decreased NO_x levels at full load by 23% at 27^o bTDC when compared with neat diesel operation. This was due to deteriorated in combustion of vegetable oil with conventional engine. LHR-2 engine with vegetable oil reduced particulate

emissions by 12% at 27° bTDC in comparison with diesel operation on same configuration of the engine. This was because of higher calorific value of diesel producing higher gas temperatures causing higher NOx levels with diesel operation.
LHR-2 engine with vegetable oil operation increased NOx emissions at full load by 77% at recommended injection timing in comparison with conventional engine with vegetable oil operation. This was due to higher heat release rate and gas temperatures with vegetable oil operation with LHR-2engine.
LHR-2 engine with vegetable oil operation increased NO_x levels at full load by 35% at recommended injection timing when compared with neat diesel operation on conventional engine. This was due to higher heat release rate with LHR-2 engine with vegetable oil operation.
NO_x emissions at full load were observed to be higher with LHR-2 engine with neat diesel at recommended injection timing. NO_x emissions at full load were observed to be lower with conventional engine with vegetable oil at recommended injection timing.
Table.4. shows data of particulate emissions and nitrogen oxide levels at full load with conventional engine and engine with LHR-2 combustion chamber at recommended injection timing with varied injector opening pressure with different operating conditions of the vegetable oil.

The data from Table.4 shows a decrease in particulate emissions at full load with increase of injector opening pressure, with different operating conditions of the vegetable oil. This was due to improvement in the fuel spray characteristics at higher injector opening pressure and increase of air entrainment, causing lower particulate emissions. Even though viscosity of vegetable oil was higher than diesel, high injector opening pressure improves spray characteristics, hence leading to a shorter physical delay period. The improved spray also leads to better mixing of fuel and air resulting in turn in fast combustion. Similar trends were noticed by earlier researchers.[20].

From Table.4. it is noted that particulate emissions decreased with preheated vegetable oil, when compared with normal temperature of the vegetable oil. This was due to i) the reduction of density of the vegetable oil, as density was directly related to smoke emissions ii) the reduction of the diffusion combustion proportion with the preheated vegetable oil, iii) the reduction of the viscosity of the vegetable oil, with which the fuel spray does not impinge on the combustion chamber walls of lower temperatures rather than it directed into the combustion chamber.

From Table.4, it is noted that nitrogen oxide (NOx) levels increased with increase of injector opening pressure with different operating conditions of vegetable oil with conventional engine. The increase in peak brake thermal efficiency was proportional to increase in injector opening pressure. Normally, improved combustion causes higher peak brake thermal efficiency due to higher combustion chamber pressure and temperature and leads to higher NO_x formation (Table.4). This is an evident proof of enhanced spray characteristics, thus improving fuel air mixture preparation and evaporation process.

However, NOx levels decreased with engine with LHR-2combustion chamber with test fuels with increase of injector opening pressure. This was due to reduction of gas temperatures with improved combustion in engine with LHR-2 combustion chamber. Similar trends were noticed by earlier researchers. [14]-[17].

NO_x levels decreased with preheating of the vegetable oil with both versions of the engine as noticed from Table.7.4. The fuel spray properties may be altered due to differences in viscosity and surface tension. The spray properties affected may include droplet size, droplet momentum, degree of mixing, penetration, and evaporation. The change in any of these properties may lead to different relative duration of premixed and diffusive combustion regimes. Since the two burning processes (premixed and diffused) have different emission formation characteristics, the change in spray properties due to preheating of the vegetable oil lead to reduction in NOx formation. As fuel temperature increased, there was an improvement in the ignition quality, which will cause shortening of ignition delay. A short ignition delay period lowers the peak combustion temperature which suppresses NOx formation. Lower levels of NO_x was also attributed to retarded injection, improved evaporation, and well mixing of preheated vegetable oil due to their viscosity at preheated temperatures. Similar trends were noticed by earlier researchers [14]-[17]

TABLE.4

DATA OF PARTICULATE EMISSIONS AND NITROGEN OXIDE (NOX) LEVELS WITH TEST FUELS

AT FULL LOAD OPERATION.

Injection timing	Test fuel	Particulate Emissions at full load operation (HSU)	NO_x Levels (ppm) at full load operation

(º bTDC)		Injector Opening Pressure (Bar)						Injector Opening Pressure (Bar)					
		190		230		270		190		230		270	
		NT	PT	NT	PT	NT	PT	NT	PT	NT	PT	NT	PT
27(CE)	DF	48	--	38	--	34	--	850		900		950	
	CJO	65	60	63	58	58	54	650	600	700	650	750	700
27(LHR-2)	DF	55	---	50	---	45	---	1250	--	1200	--	1150	---
	CJO	40	35	35	30	30	25	1100	1050	1050	1000	1000	950

4.CONCLUSION

1. **Engine with LHR-2 combustion chamber consisted of air gap insulated piston with superni (an alloy of nickel) crown, and air gap insulated liner with vegetable oil opertoin showed reduction of particulate emissions and increase of nitrogen oxide levels at full load at 27º bTDC in comparison with conventional engine with vegetable oil operation and diesel operation at 27º bTDC.**
2. **Engine with LHR-2 combustion chamber with vegetable oil opertoin showed reduction of particulate emissions and nitrogen oxide levels at 27 º bTDC in comparison with same configuration of the engine wth diesel oeparion**
3. **Exhasut emissions improved marginally with an increase of injector opeining pressure with vegetable ol operation with both versions of the combustion chamber.**

4.1 Research Findings and Suggestions

Comparative studies on exhaust emissions with direct injection diesel engine with LHR–3 combustion chamber and conventional combustion chamber were made at varied injection pressure with neat vegetable oil operaion. LHR-2 engine increased drastically NOx emissions. Hence, NOx levels can be reduced with selective catalytic reduction technique. [21].

4.2 Future Scope of Work

Hence further work on the effect of injection timing with engine with LHR–3 combustion chamber with vegetable oil operation is necessary. Studies on exhaust emissions with varied injection timing and injection pressure with vegetable oil operation on engine with LHR-2 combustion chamber can be taken up.

ACKNOWLEDGMENTS

Authors thank authorities of Chaitanya Bharathi Institute of Technology, Hyderabad for providing facilities for carrying out this research work. Financial assistance provided by All India Council for Technical Education (AICTE), New Delhi, is greatly acknowledged.

REFERENCES:

1. Avinash Kumar Agarwal and Atul Dha. "Performance, emission and combustion characteristics of jatropha oil blends in a direct injection CI engine," SAE Paper 2009–01–0947.
2. R.D. Misra, M.S. Murthy, " Straight vegetable oils usage in a compression ignition engine—A review," Renew Sustain Energy Rev, 14, pp. 3005–3013,,2010.
3. **No. Soo-Young,"Inedible vegetable oils and their derivatives for alternative diesel fuels in CI engines: A review," Renew Sustain Energy Rev, 15, pp. 131–149,2011.**
4. Avinash Kumar Agarwal and Atul Dhar. "Experimental investigations of performance, emission and combustion characteristics of Karanja oil blends fuelled DICI engine," Renewable Energy , 52, pp. 283–291,2013.
5. N. Venkateswara Rao, M.V.S. Murali Krishna, and P.V.K. Murthy, " Comparative studies on performance of tobacco seed oil in crude form and biodiesel form in direct injection diesel engine," *Int J Aut Eng Res & Dev*, 3 (4), pp. 57–72,2013.
6. **D. Srikanth, M.V.S. Murali Krishna and P. Ushasri, "Performance evaluation of a diesel engine fuelled with cotton seed oil in crude form and biodiesel form," Int J Acad Res Multidiscip, 1 (9), pp. 329–349,2013.**
7. **Maddali Krishna, and R. Chowdary, "Comparative studies on performance evaluation of waste fried vegetable oil in crude form and biodiesel form in conventional diesel engine," SAE Paper 2014–01–1947, 2014.**
8. N.Durga Prasada Rao, M.V.S. Murali Krishna, and B. Anjeneya Prasad, " Effect of injector opening pressure and injection timing on exhaust emissions and combustion characteristics of rice bran oil in crude form and biodiesel form in direct injection diesel engine, ", IOSR J Eng, 4(2), pp.9–19,2014.
9. I.Celikten, "An experimental investigation of the effect of the injection pressure on the engine performance and exhaust emission in indirect injection diesel engines," *Applied Thermal Engineering*, **23**, pp.2051–2060,2003.
10. Y.Cingur, *and D.* Altiparmak, " Effect of cetane number and injection pressure on a DI diesel engine performance and emissions," *Energy Conversion and Management*, **44**, pp. 389–397,2003.
11. D.T. Hountalas, D.A. Kouremenos, K.B.Binder, V. Schwarz, V. and G.C. Mavropoulos, " Effect of injection pressure on the performance and exhaust emissions of a heavy duty DI diesel engine," *SAE Technical Paper No. 2003-01-0340. Warrendale, PA,2003.*
12. S.Jindal, B.P. Nandwana, N.S. Rathore, and V. Vashistha, "Experimental investigation of the effect of compression ratio and injector opening pressure in a direct injection diesel engine running on Jatropha methyl ester,"*Applied Thermal Engineering*, **30**,442–448,2010.
13. Avinash Kumar Agarwal, Dhananjay Kumar Srivastava, Atul Dhar, et al. "Effect of fuel injection timing and pressure on combustion, emissions and performance characteristics of a single cylinder diesel engine," *Fuel*, 111, pp. 374–83,2013.
14. **Ch. Chennakesava Reddy, M.V.S. Murali Krishna,P.V.K. Murthy,and T. Ratna Reddy, "Potential of low heat rejection diesel engine with crude pongamia oil," *International Journal of Modern Engineering Research*, 1(1), pp.*210-224,2011.***
15. N. Janardhan,M.V.S. Murali Krishna, P.Ushasri, P.V.K. Murthy, "Potential of a medium low heat rejection diesel engine with crude jatropha oil," *International Journal of Automotive Engineering and Technologies, 1(2), pp.1-16,2012.*
16. N. Janardhan,M.V.S. Murali Krishna, P.Ushasri, P.V.K. Murthy, "Comparative performance, emissions and combustion characteristics of jatropha oil in crude form and biodiesel form in a medium grade low heat rejection diesel engine," *International Journal of Soft Computing and Engineering, 2(5),pp.5-15,2013.*
17. **D. Srikanth, M.V.S. Murali Krishna, P.Ushasri, and P.V.Krishna Murthy, "Comparative studies on medium grade low heat rejection diesel engine and conventional diesel engine with crude cotton seed oil," *International Journal of Innovative Research in Science, Engineering and Technology, 2(10), pp.5809-5228,,2013.***
18. M.V.S. Murali Krishna, "Performance evalution of LHR diesel engine with alternative fuels," PhD Thesis, JNT University, Hyderabad, India,2004.
19. K. Rama Mohan, C.M. Vara Prasad, and M.V.S. Murali Krishna, "Performance of a low heat rejection diesel engine with air gap insulated piston," ASME J Gas Turbines and Power, 121 (3), pp. 530–540,1999.
20. Avinash Kumar Agarwal, Dhananjay Kumar Srivastava, Atul Dhar, et al. "Effect of fuel injection timing and pressure on combustion, emissions and performance characteristics of a single cylinder diesel engine," Fuel, 111, pp.374–83,2013.
21. N. Janardhan, P. Ushasri , M.V.S.Murali Krishna and P.V.K. Murthy, "Performance of biodiesel in low heat rejection diesel engine with catalytic converter. *International Journal of Engineering and Advanced Technology2(2), 97-109, 2012.*

EFFECT OF INJECTION TIMING ON EXHAUST EMISSIONS AND COMBUSTION CHARACTERISTICS OF DIRECT INJECTION DIESEL ENGINE WITH AIR GAP INSULATION

N. Janardhan[1]

[1]Mechanical Engineering Department, Chaitanya Bharathi Institute of Technology,

Gandipet, Hyderabad 500 075, Telangana State, India,

[1]E-mail: narambhatlu.datta@gmail.com,

***Abstract**:* Experiments were carried out to study exhaust emissions of diesel engine with air gap insulated low heat rejection (LHR–2) combustion chamber consisting of air gap insulated piston with 3 mm air gap, with superni (an alloy of nickel) crown, air gap insulated liner with superni insert with neat diesel with varied injection timing. Exhaust emissions of particulate emissions and nitrogen oxide (NO_x) levels were determined at various values of brake mean effective pressure (BMEP) of the LHR-2 combustion chamber and compared with neat diesel operation on conventional engine (CE) at similar operating conditions. Combustion diagnosis was carried out using miniature Piezo electric pressure transducer, TDC (top dead centre) and special pressure-crank angle software package at full load operation. The optimum injection timing was found to be 31^{o}bTDC (before top dead centre) with conventional engine, while it was 29^o bTDC for engine with LHR–2 combustion chamber with diesel operation. Engine with LHR–2 combustion chamber with neat diesel operation showed increased particulate emissions and NOx levels at manufacturer's recommended injection timing of 27^o bTDC, and the they improved marginally with advanced injection timing of 31^{o}bTDC in comparison with CE at 27^{o}bTDC.

***Keywords*:** Conservation of diesel, conventional engine, LHR combustion chamber, Performance.

I.INTRODUCTION

In the scenario of i) increase of vehicle population at an alarming rate due to advancement of civilization, ii) use of diesel fuel in not only transport sector but also in agriculture sector leading to fast depletion of diesel fuels and iii) increase of fuel prices in International market leading to burden on economic sector of Govt. of India, the conservation of diesel fuel has become pertinent for the engine manufacturers, users and researchers involved in the combustion research. [1].

The nation should pay gratitude towards Dr. Diesel for his remarkable invention of diesel engine. Compression ignition (CI) engines, due to their excellent fuel efficiency and durability, have become popular power plants for automotive applications. This is globally the most accepted type of internal combustion engine used for powering agricultural implements, industrial applications, and construction equipment along with marine propulsion. [2–3].

The concept of LHR combustion chamber is to reduce coolant losses by providing thermal resistance in the path of heat flow to the coolant, there by gaining thermal efficiency. Several methods adopted for achieving LHR to the coolant are ceramic coated engines and air gap insulated engines with creating air gap in the piston and other components with low-thermal conductivity materials like superni, cast iron and mild steel etc.

LHR combustion chambers were classified as ceramic coated (LHR–1), air gap insulated (LHR–2) and combination of ceramic coated and air gap insulated engines(LHR-3) combustion chambers depending on degree of insulations.

Wallace et al. also studied the performance of the insulated piston engine in which air gap thickness was maintained at 2-mm. [4]. The major finding was increase of particulate emissions due to reduction of air–fuel ratios from 18.27 to astonishingly small 12.76, which was inadmissible in practice.

Karthikeyan et al. studied the performance of a diesel engine by insulating engine parts employing 2-mm air gap in the piston and the liner, thus attaining a semi-adiabatic condition. [5]. The nimonic piston with 2-mm air gap was studded with the body of the piston. Mild steel sleeve, provided with 2-mm air gap was fitted with the total length of the liner. They reported increase of particulate emissions at all loads, when compared to neat diesel operation on conventional engine. This was due to higher exhaust gas temperatures.

Jabez Dhinagar et al. conducted experiments on LHR engine, with an air gap insulated piston, air gap insulated liner and ceramic coated cylinder head. [6]. The piston with nimonic crown with 2 mm air gap was fitted with the body of the piston by stud design.

Mild steel sleeve was provided with 2 mm air gap and it was fitted with the 50 mm length of the liner. The performance was deteriorated with this engine and increase of particulate emissions at full load operation with neat diesel operation, at recommended injection timing. Hence the injection timing was retarded to improve performance and pollution levels.

The technique of providing an air gap in the piston involved the complications of joining two different metals. Investigations were carried out on LHR–2 combustion chamber- with air gap insulated piston with pure diesel.[7]. However, the bolted design employed by them could not provide complete sealing of air in the air gap. Investigations were carried out with engine with LHR–2 combustion chamber with air gap insulated piston with nimonic crown threaded with the body of the piston fuelled with neat diesel with varied injection timing. It was reported from their investigations that particulate emissions and NO_x levels decreased and improved combustion characteristics with advanced injection timing of 29.5º bTDC Engine with LHR combustion chamber was more suitable for vegetable oil operation, as hot combustion chamber was maintained by it in burning high viscous vegetable oils. Experiments were conducted on engine with LHR–2 combustion chamber with varied injection timing and injection pressure. [9–14]. It was reported from their investigations that engine with LHR-2 combustion chamber decreased particulate emissions by 8-10% in comparison with neat diesel operation on CE. Exhaust emissions and combustion characteristics were improved with advanced injection timing.

The present paper attempted to evaluate the performance of medium grade LHR combustion chamber, which consisted of air gap insulated piston and air gap insulated liner. This medium grade LHR–2 combustion chamber was fuelled with diesel fuel with varied injection timing. Comparative performance studies were made on engine with LHR–2 combustion chamber with conventional engine with diesel operation.

MATERIALS AND METHODS

This part deals with fabrication of air gap insulated piston and air gap insulated liner, brief description of experimental set-up, specification of experimental engine, operating conditions and definitions of used values.

The physic-chemical properties of the diesel fuel are presented in Table-1.

Table.1. Properties Of Diesel

Property	Units	Diesel
Carbon chain	--	C_8-C_{28}
Cetane Number		55
Density	gm/cc	0.84
Bulk modulus @ 20Mpa	Mpa	1475
Kinematic viscosity @ 40ºC	cSt	2.25
Sulfur	%	0.25
Oxygen	%	0.3
Air fuel ratio (stochiometric)	--	14.86
Lower calorific value	kJ/kg	44800
Flash point (Open cup)	ºC	68
Molecular weight	--	226
Colour	--	Light yellow

LHR-2 combustion chamber (Fig.1) contained a two-part piston; the top crown made of low thermal conductivity material, superni–90 (an alloy of nickel) screwed to aluminum body of the piston, providing a 3 mm air gap in between the crown and the body of the piston. The optimum thickness of air gap in the air gap piston was found to be 3-mm for improved performance of the engine with diesel as fuel. [8]. The height of the piston was maintained such that compression ratio was not altered.

A superni-90 insert was screwed to the top portion of the liner in such a manner that an air gap of 3-mm was maintained between the insert and the liner body. At 500ºC the thermal conductivity of superni-90 and air are 20.92 and 0.057 W/m-K.

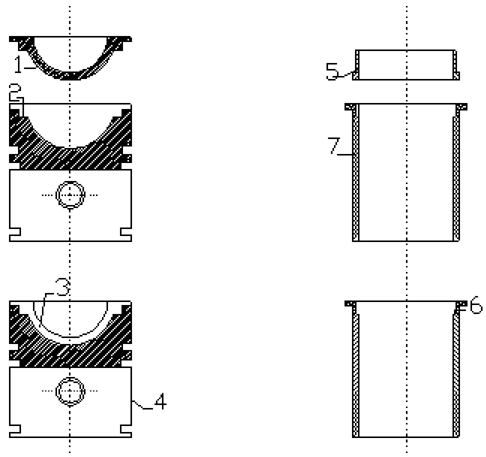

1 Superni crown with threads, 2 Superni gasket , 3.Air gap in piston, 4. Body of the piston, 5 Superni insert with threads , 6 Air gap in liner, 7. Body of the liner

Fig.1. Assembly details of air gap insulated piston and air gap insulated liner

The test fuel used in the experimentation was neat diesel. The schematic diagram of the experimental setup with diesel operation is shown in Figure 2. The specifications of the experimental engine are shown in Table-2. Experimental setup used for study of exhaust emissions on low grade LHR diesel engine with cottonseed biodiesel in Fig.3 The specification of the experimental engine (Part No.1) is shown in Table.2 The engine was connected to an electric dynamometer (Part No.2. Kirloskar make) for measuring its brake power. Dynamometer was loaded by loading rheostat (Part No.3). The combustion chamber consisted of a direct injection type with no special arrangement for swirling motion of air. Burette (Part No.9) method was used for finding fuel consumption of the engine with the help of fuel tank (Part No7) and three way valve (Part No.8). Air-consumption of the engine was measured by air-box method consisting of an orifice meter (Part No.4), U-tube water manometer (Part No.5) and air box (Part No.6) assembly.

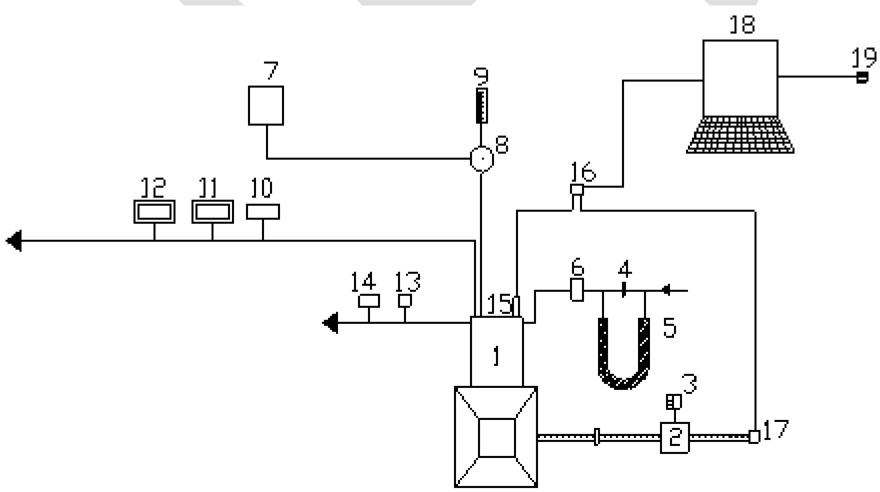

1.Engine, 2.Electical Dynamometer, 3.Load Box, 4.Orifice flow meter, 5.U-tube water manometer, 6.Air box, 7.Fuel tank, 8, Three way valve 9.Burette, 10. Exhaust gas temperature indicator, 11.Smoke opacity meter, 12.NO_x Analyzer, 13.Outlet–jacket water temperature indicator, 14. Outlet-jacket water flow meter, 15. Piezo-electric pressure transducer, 16.Console, 17.TDC encoder, 18.Personal Computer and 19. Printer.

Fig.2 Schematic diagram of experimental set–up

The naturally aspirated engine was provided with water-cooling system in which outlet temperature of water is maintained at 80ºC by adjusting the water flow rate. Engine oil was provided with a pressure feed system. No temperature control was incorporated, for measuring the lube oil temperature.

Table.2. Specifications of the Test Engine

Description	Specification
Engine make and model	Kirloskar (India) AV1
Maximum power output at a speed of 1500 rpm	3.68 kW
Number of cylinders ×cylinder position× stroke	One × Vertical position × four-stroke
Bore × stroke	80 mm × 110 mm
Method of cooling	Water cooled
Rated speed (constant)	1500 rpm
Fuel injection system	In-line and direct injection
Compression ratio	16:1
BMEP @ 1500 rpm	5.31 bar
Manufacturer's recommended injection timing and pressure	27ºbTDC × 190 bar
Dynamometer	Electrical dynamometer
Number of holes of injector and size	Three × 0.25 mm
Type of combustion chamber	Direct injection type
Fuel injection nozzle	Make: MICO-BOSCH No- 0431-202-120/HB
Fuel injection pump	Make: BOSCH: NO- 8085587/1

The naturally aspirated engine was provided with water-cooling system in which outlet temperature of water is maintained at 80ºC by adjusting the water flow rate, which was measured by water flow meter (Part No.14). Exhaust gas temperature (EGT) and coolant water outlet temperatures were measured with thermocouples made of iron and iron-constantan attached to the exhaust gas temperature indicator (Part No.10) and outlet jacket temperature indicator (Part No.13). Copper shims of suitable size were provided in between the pump body and the engine frame, to vary the injection timing and its effect on the exhaust emissions and combustion characteristics of the engine was studied

Exhaust emissions of particulate matter and nitrogen oxides (NO_x) were recorded by smoke opacity meter (AVL India, 437) and NO_x Analyzer (Netel India ;4000 VM) at full load operation of the engine. Table 3 shows the measurement principle, accuracy and repeatability of raw exhaust gas emission analyzers/ measuring equipment for particulate emissions and NO_x levels. Analyzers were allowed to adjust their zero point before each measurement. To ensure that accuracy of measured values was high, the gas analyzers were calibrated before each measurement using reference gases.

Table.3

Specifications of the

Smoke Opacimeter (AVL, India, 437). And NO_x Analyzer (Netel India, (4000 VM))

Pollutant	Measuring Principle	Range	Least Count	Repeatability
Particulate Emissions	Light extinction	1–100%	0.1% of Full Scale (FS)	0.1% for 30 minutes
NO_x	Chemiluminiscence	1–5000 ppm	0.5% of FS	≤0.5% F.S

Water cooled Piezo electric transducer(AVL Austria: QC34D)., fitted on the cylinder head to measure pressure in the combustion chamber was connected to a console, which in turn was connected to Pentium personal computer. TDC (top dead centre) encoder (AVL Austria: 365x) with a crank angle (CA) resolution of 0.5 crank angle degrees (CAD) provided at the extended shaft of the dynamometer was connected to the console to determine the crankshaft position. A special pressure-crank angle (P–θ) software package evaluated the combustion characteristics such as peak pressure (PP), time of occurrence of peak pressure (TOPP) and maximum rate of pressure rise (MRPR) from the signals of pressure and crank angle at the peak load operation of the engine. Pressure-crank angle diagram was obtained on the screen of the personal computer.

Operating Conditions: Fuel used in experiment was neat diesel. Various injection timings attempted in the investigations were 27–34°bTDC.

3. RESULTS AND DICUSSION

3.1.Performance Parameters

The variation of brake thermal efficiency (BTE) with brake mean effective pressure (BMEP) in the conventional engine (CE) with pure diesel, at various injection timings at an injector opening pressure of 190 bar, is shown in Fig. 3.

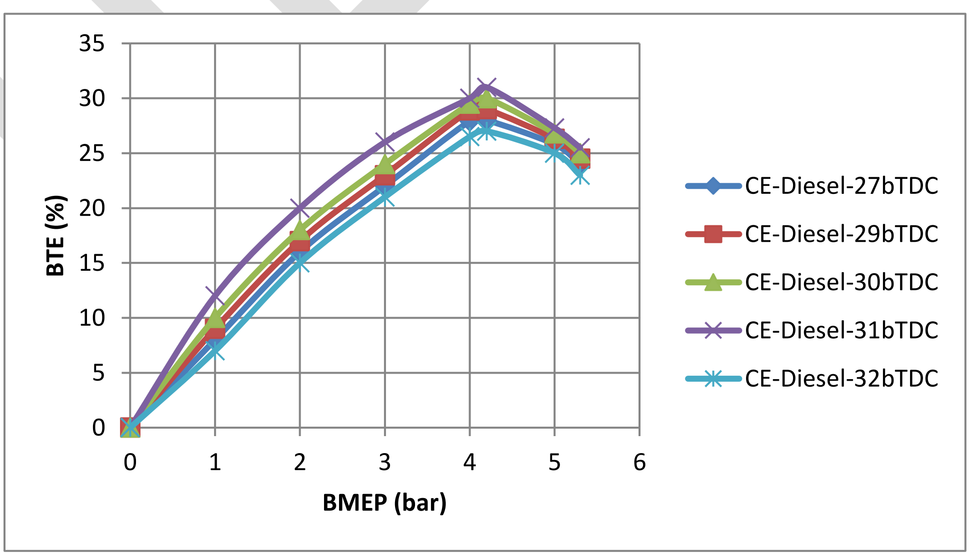

Fig.3 variation of brake thermal efficiency (BTE) with brake mean effective pressure (BMEP) in the conventional engine with neat diesel, at various injection timings at an injector opening pressure of 190 bar.

BTE increased with the advanced injection timings in the conventional engine at all loads, due to early initiation of combustion and increase of contact period of fuel with air leading to improve air fuel ratios period. The optimum injection timing was obtained by based on maximum brake thermal efficiency. Maximum BTE was observed when the injection timing was advanced to 31°bTDC in CE. Performance deteriorated if the injection timing was greater than 31°bTDC. This was because of increase of ignition delay.

The variation of BTE with BMEP in the LHR–2 combustion chamber with neat diesel at various injection timings at an injector opening pressure of 190 bar, is shown in Fig. 4

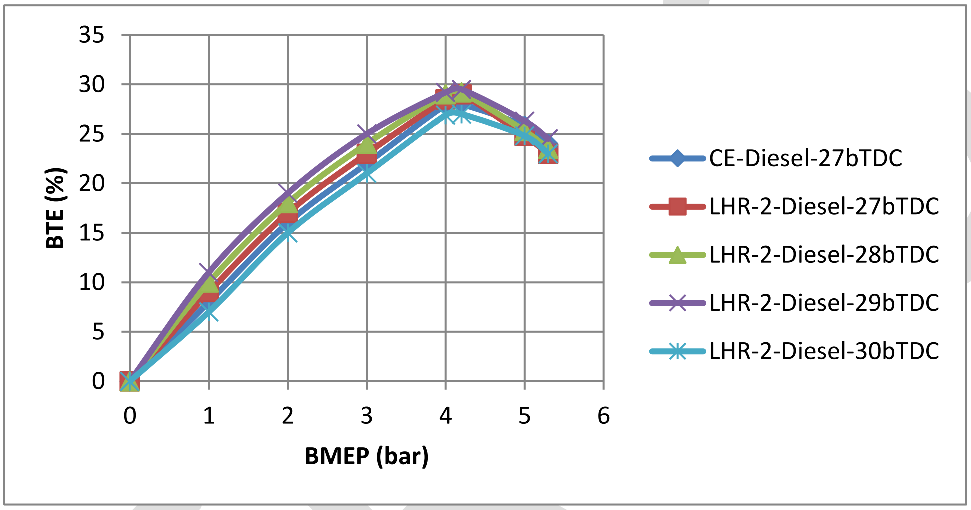

Fig.3 variation of brake thermal efficiency (BTE) with brake mean effective pressure (BMEP) in the engine with LHR–2 combustion chamber with neat diesel, at various injection timings at an injector opening pressure of 190 bar.

BTE increased up to 80% of the full load in the LHR–2 combustion chamber at the recommended injection timing and beyond this load, it decreased over and above that of the conventional engine. As the combustion chamber was insulated to greater extent, it was expected that high combustion temperatures would be prevalent in LHR engine. It tends to decrease the ignition delay thereby reducing pre-mixed combustion as a result of which, less time was available for proper mixing of air and fuel in the combustion chamber leading to incomplete combustion, with which BTE decreased beyond 80% of the full load. More over at this load, friction and increased diffusion combustion resulted from reduced ignition delay. Increased radiation losses might have also contributed to the deterioration. Higher value of BTE at all loads including 100% full load was observed when the injection timing was advanced to 29° bTDC in the LHR–2 combustion chamber. Further advancing of the injection timing resulted in increase in fuel consumption due to longer ignition delay. Hence it was concluded that the optimized performance of the LHR-2 combustion chamber was achieved at an injection timing of 29°bTDC.

3.2 Exhaust Emissions

Particulate emissions and nitrogen oxide (NOx) levels are the emissions from diesel engine cause health hazards like inhaling of these pollutants cause severe headache, tuberculosis, lung cancer, nausea, respiratory problems, skin cancer, hemorrhage, etc. [15–17]. The contaminated air containing carbon dioxide released from automobiles reaches ocean in the form of acid rain, there by polluting water. Hence control of these emissions is an immediate task and important.

A rich fuel–air mixture resulted in higher smoke because of the availability of oxygen was less. Fig.4 indicates that particulate emissions increased from no load to full load in both versions of the combustion chamber. During the first part, the smoke level was more or less constant, as there was always excess air present. However, in the higher load range there was an abrupt rise in smoke levels due to less available oxygen, causing the decrease of air-fuel ratio, leading to incomplete combustion, producing more soot density. The variation of smoke levels with the BMEP, typically showed a inverted L-shaped behavior

due to the pre-dominance of hydrocarbons in their composition at light load and of carbon at high load. Up to 80% of full load, marginal reduction of particulate emissions was observed in the engine with LHR–2 combustion chamber, when compared to the conventional engine. This was due to the increased oxidation rate of soot in relation to soot formation. Higher surface temperatures of engine with LHR–2 combustion chamber aided this process. Soot formation and buildup in the engine cylinder was also a very important consideration. Soot is formed during combustion in low oxygen regions of the flames. Engine with LHR–2 combustion chamber shorten the delay period, which curbs thermal cracking, responsible for soot formation.

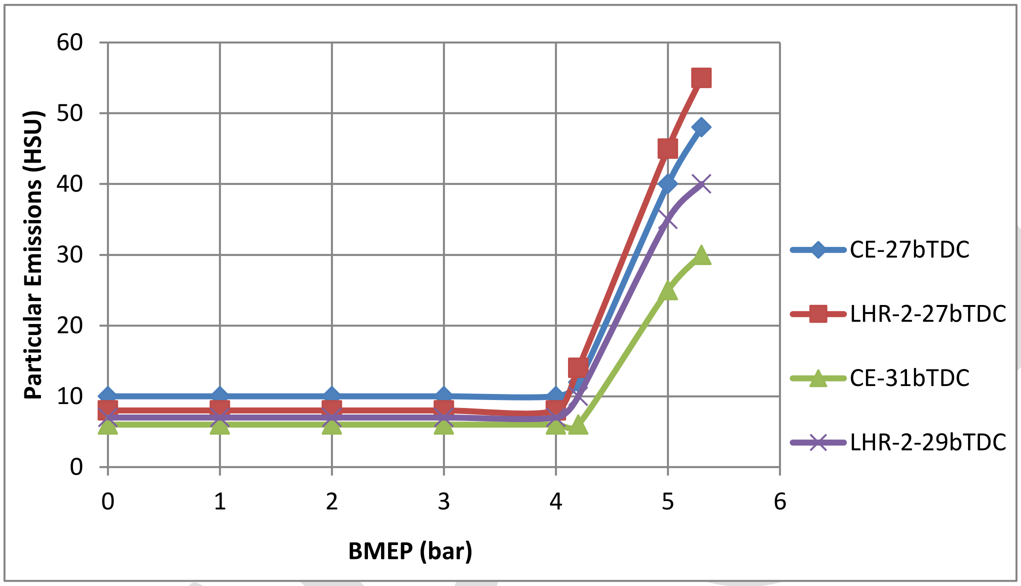

Fig.4. Variation of particular emissions in Hartridge Smoke Unit (HSU) with brake mean effective pressure (BMEP) in conventional engine (CE) and engine with LHR-2 combustion chamber at recommended injection timing and at optimized injection timing at an injector opening pressure of 190 bar.

Beyond 80% of full load, marginal and slight increase of particulate emissions was observed in the LHR-2 combustion chamber, when compared to conventional engine. This was due to fuel cracking at higher temperature, leading to increase in smoke density. Higher temperature of LHR–2 combustion chamber produced increased rates of both soot formation and burn up. The reduction in volumetric efficiency and air-fuel ratio were responsible factors for increasing particulate emissions in the engine with LHR–2 combustion chamber near the full load operation of the engine. As expected, smoke increased in the LHR–2 combustion chamber because of higher temperatures and improper utilization of the fuel consequent upon predominant diffusion combustion. Particulate emissions decreased with advanced injection timing at all loads with engine with both versions of the combustion chamber. This was due to increase of contact period with fuel with air and thus improving atomization characteristics in both versions of the combustion chamber. Higher combustion temperatures are also conducive for reducing particulate emissions. Fuel cracking reactions were eliminated with LHR–2 combustion chamber due to low combustion temperatures. This confirmed improvement in fuel utilization with the injection timing of 29^{o} bTDC. Rama Mohan also observed the similar trends.[7]

Fig.5 indicates that engine with LHR-2 combustion chamber increased particulate emissions at full load by 25% at 27^{o} bTDC and 33% at 29^{o} bTDC in comparison with CE at 27^{o} bTDC and 31^{o} bTDC. This was due to reduction of ignition delay with engine with LHR–2 combustion chamber at 27^{o} bTDC and increased injection timing advance with CE in comparison with insulated engine.

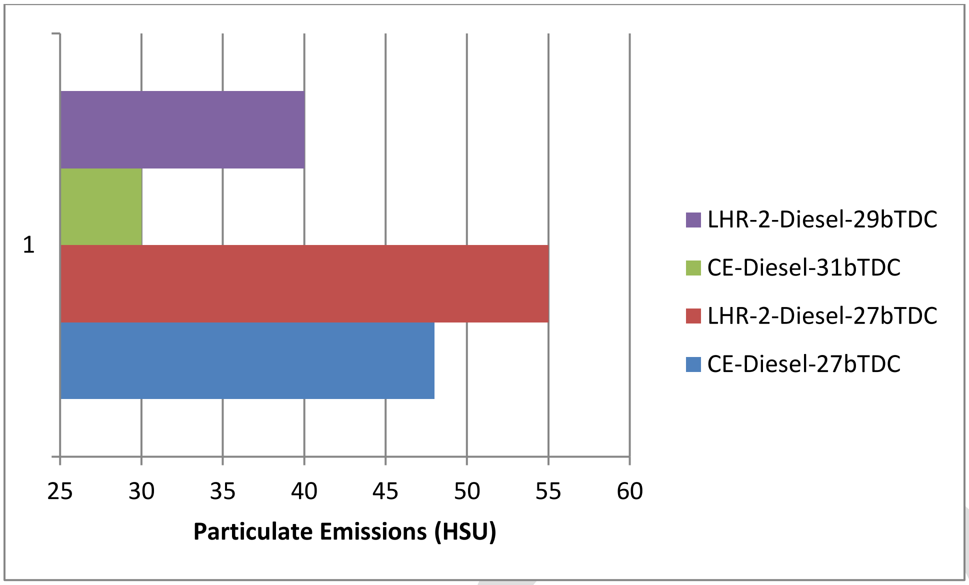

Fig.5. Bar charts showing the variation of particulate emissions at full load with injection timing with both versions of the combustion chamber

The temperature and availability of oxygen are the reasons for the formation of NO_x. For both versions of the combustion chamber, Fig.6 indicates that NO_x concentrations raised steadily as the fuel/air ratio increased with increasing BP/BMEP, at constant injection timing.

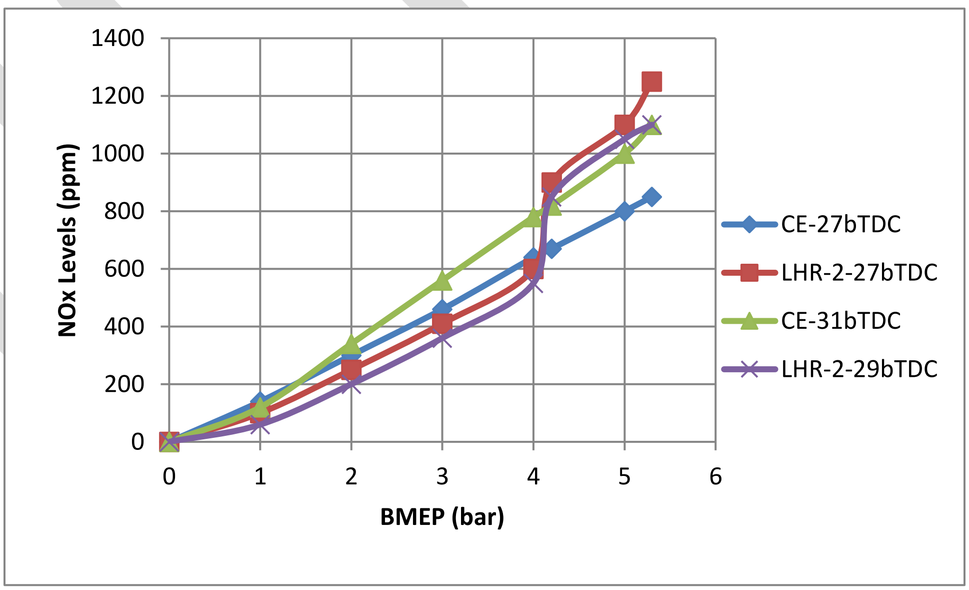

Fig.6. Variation of nitrogen oxide (NO_x) levels with brake mean effective pressure (BMEP) in conventional engine (CE) and engine with LHR-2 combustion chamber at recommended injection timing and at optimized injection timing at an injector opening pressure of 190 bar.

At part load, NO_x concentrations were less in both versions of the engine. This was due to the availability of excess oxygen. At remaining loads, NOx concentrations steadily increased with the load in both versions of the combustion chamber. This was because, local NO_x concentrations raised from the residual gas value following the start of combustion, to a peak at the point where the local burned gas equivalence ratio changed from lean to rich. At full load, with higher peak pressures, and hence temperatures, and larger regions of close-to-stoichiometric burned gas, NO_x levels increased in both versions of the engine. Though amount of fuel injected decreased proportionally as the overall equivalence ratio was decreased, much of the fuel still burns close to stoichiometric. Thus NO_x emissions should be roughly proportional to the mass of fuel injected (provided burned gas pressures and temperature do not change greatly).

The LHR-2 combustion chamber recorded lower NOx levels up to 80% of the full load, and beyond that load it produced higher NOx levels compared to conventional engine. As the air-fuel ratios were higher in the LHR-2 combustion chamber, causing more dilution, due to mixing with the excess air, leading to produce less NOx concentrations, up to 80% of the full load, when compared to CE. Beyond 80% of full load, due to the reduction of fuel-air equivalence ratio with LHR–2 combustion chamber, which was approaching to the stoichiometric ratio, causing higher value of NOx levels. NOx emissions increased with advanced injection timing with CE. Increasing the injection advance resulted in higher combustion temperatures and increase of resident time leading to produce higher value of NOx levels in the exhaust of conventional engine at its optimum injection timing. However, NOx levels decreased with advanced injection timing with engine with LHR-2 combustion chamber with diesel. This was due to decrease of combustion temperatures with improved air fuel ratios. Rama Mohan reported the similar trend with NO_x emissions in the LHR engine at the recommended and optimum injection timings.[8].

Fig.7 indicates that engine with LHR-2 combustion chamber increased NO_x levels by 45% at 27° bTDC and comparable at 29° bTDC when compared with CE at 27° bTDC and at 31° bTDC. This was due to increase of peak pressures in the LHR-2 combustion chamber at 27° bTDC and resident time with CE.

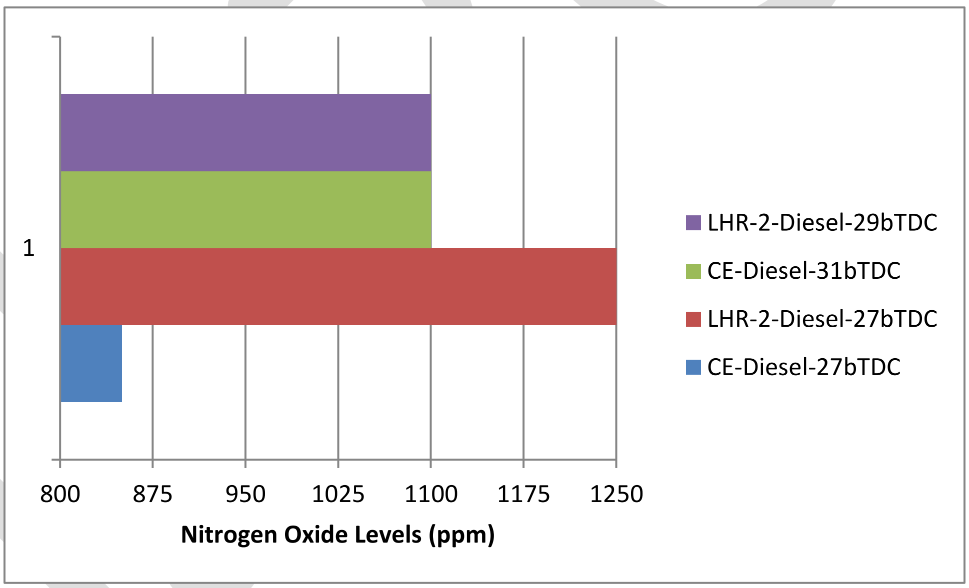

Fig.7 Bar charts showing the variation of nitrogen oxide levels (NO_x) at full load with injection timing with both versions of the combustion chamber

3.3 Combustion Characteristics

From Fig. 8, it is observed that peak pressure at full load operation increased with engine with LHR-2 combustion chamber at 27°bTDC in comparison with CE. This was due to high explosion of charge in hot environment provided by LHR combustion chamber. This was also because the LHR-2combustion chamber exhibited higher temperatures of combustion chamber walls leading to continuation of combustion, giving rise higher peak pressures. PP increased with CE, while decreasing the same with engine with LHR-2 combustion chamber with advanced injection timings. This was due to explosion of accumulated charge with increase of ignition delay with CE, and improved combustion with improved air fuel ratios with which gas temperatures and peak pressures decreased in LHR-2 version of the combustion chamber. Increase of NO_x emissions with CE and decrease the same with engine with LHR-2 combustion chamber with advanced injection timings established the fact that PP at full load operation increased with CE, while decreasing the same with insulated engine with advanced injection timing. Engine with LHR-2 combustion chamber increased peak pressure at full load by 20% at 27° bTDC and 7% at 29° bTDC when compared with CE at 27° bTDC and at 31° bTDC.

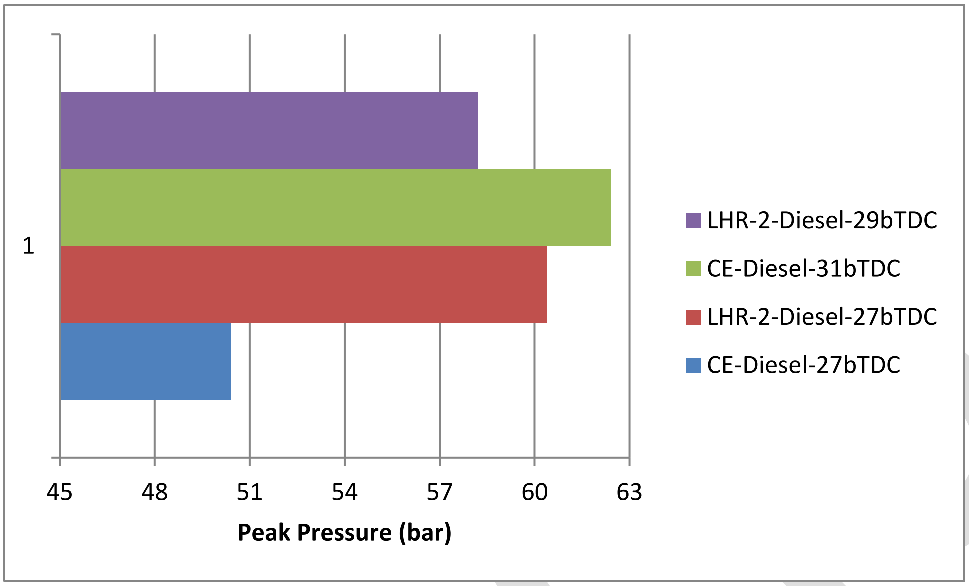

Fig.8 Bar charts showing the variation of peak pressure at full load with injection timing with both versions of the combustion chamber

Fig.9 indicates that Maximum rate of pressure raise (MRPR) at full load followed the similar trends with peak pressure in both versions of the combustion chamber. The trends observed by the authors on the aspect of MRPR in LHR-2 combustion chamber agreed well with the findings of Rama Mohan at the recommended injection timing.[8]. Engine with LHR-2 combustion chamber increased MRPR at full load by 33% at 27° bTDC and 13% at 29° bTDC when compared with CE at 27° bTDC and at 31° bTDC. This was due to reduction of ignition delay with insulated engine.

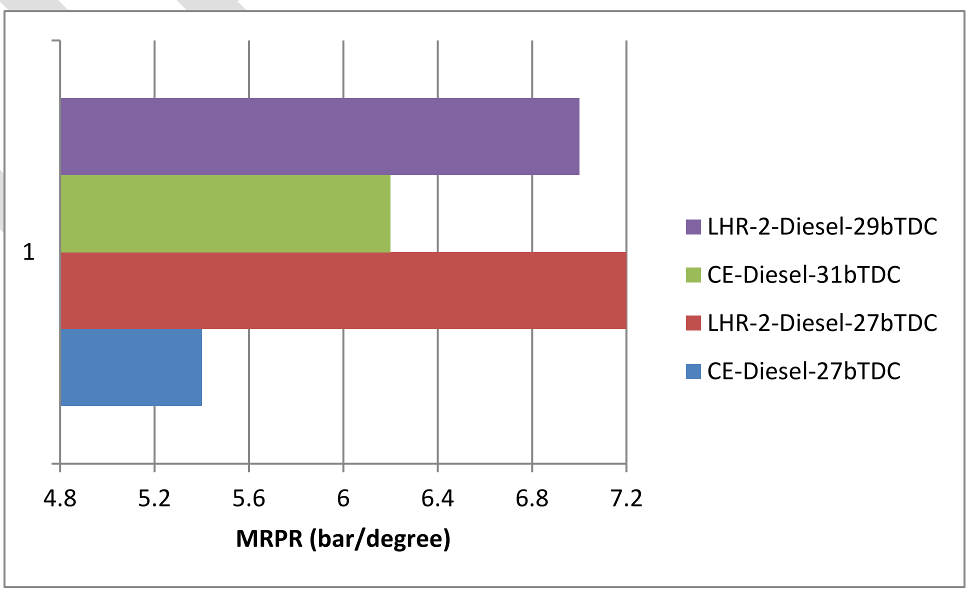

Fig.9 Bar charts showing the variation of maximum rate of pressure rise (MRPR) at full load with injection timing with both versions of the combustion chamber

From Fig.10, it is observed that time of occurrence of peak pressure (TOPP) at full load decreased (shifted towards TDC) with the advanced injection timing and in both versions of the combustion chamber. This was confirmed that both versions of the combustion chamber showed improvement in performance, when the injection timings were advanced to their optimum values. Engine with LHR-2 combustion chamber increased TOPP at full load by 11% at 27° bTDC and 12% at 29° bTDC when compared with CE at 27° bTDC and at 31° bTDC. This was due to continuation of combustion with hot insulated components of LHR-2 combustion chamber giving TOPP away from TDC in comparison with CE. .

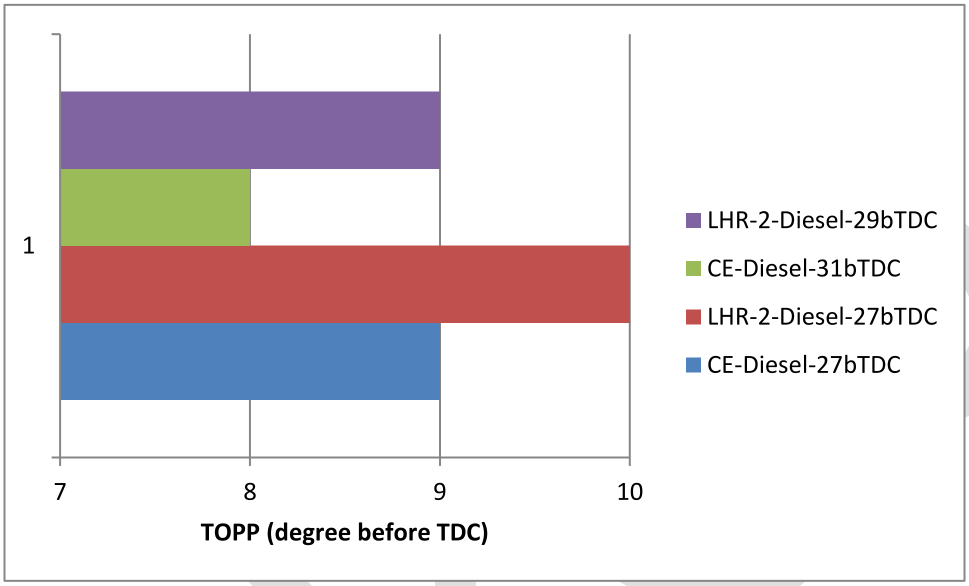

Fig.10 Bar charts showing the variation of time of occurrence of peak pressure (TOPP) at full load with injection timing with both versions of the combustion chamber

4. CONCLUSIONS

4. **Engine with LHR-2 combustion chamber showed improved exhaust emissions of particulate emissions and NO_x levels at 80% of the full load operation at 27 °bTDC in comparison with conventional engine at 27 °bTDC.**
5. **Engine with LHR-2 combustion chamber showed increased particulate emissions and NOx levels at the full load operation at 27 °bTDC in comparison with conventional engine at 27 °bTDC.**
6. **At full load operation, engine with LHR-2 combustion chamber at 29° bTDC, decreased particulate emissions by 27%, NOx levels by 12% , decreased peak pressure by 3%, MRPR by 3% and TOPP by 10% in comparison with same configuration of combustion chamber at an injection timing of 27 °bTDC.**
7. **AT full load operation, conventional engine at 31° bTDC, decreased particulate emissions by 38%, NOx levels by 29%, peak pressure by 24%, MRPR by 15% and decreased TOPP by 11% in comparison with CE at an injection timing of 27 °bTDC.**

4.1 Research Findings

Comparative studies on exhaust emissions and combustion characteristic with direct injection diesel engine with LHR–2 combustion chamber and conventional combustion chamber were determined at varied injection timing with neat diesel operation.

4.2 Future Scope of Work

Hence further work on the effect of injector opening on pressure with engine with LHR–2 combustion chamber with diesel operation is necessary. Studies on performance parameters with varied injection timing and injection pressure with neat diesel operation on engine with LHR-2 combustion chamber can be taken up.

ACKNOWLEDGMENTS

Authors thank authorities of Chaitanya Bharathi Institute of Technology, Hyderabad for providing facilities for carrying out this research work. Financial assistance provided by All India Council for Technical Education (AICTE), New Delhi, is greatly acknowledged.

REFERENCES:

1. Matthias Lamping, Thomas Körfer, Thorsten Schnorbus, Stefan Pischinger, Yunji Chen : Tomorrows Diesel Fuel Diversity – Challenges and Solutions, SAE 2008-01—1731
2. Cummins, C. and Jr. Lyle Diesel's Engine, Volume 1: From Conception To 1918”. Wilsonville, OR, USA: Carnot Press, ISBN 978-0-917308-03-1, 1993.
3. Avinash Kumar Agarwal,Dhananjay Kumar Srivastava , Atul Dhar, Rakesh Kumar Maurya, Pravesh Chandra Shukla, Akhilendra Pratap Singh.(2013), Effect of fuel injection timing and pressure on combustion, emissions and performance characteristics of a single cylinder diesel engine, *Fuel*, 111 pp 374–383.
4. Wallace, F.J., Kao, T.K., Alexander, W.D., Cole, A. and Tarabad, M. (1983), Thermal barrier piston and their effect on the performance of compound diesel engine cycles, SAE Paper No. 830312, 1983.
5. Karthikeyan, S., Arunachalam, M., Srinivasan Rao, P. and Gopala Krishanan, K.V. (1985), Performance of an alcohol, diesel oil dual-fuel engine with insulated engine parts”, Proceedings of 9th National Conference of I.C. Engines and Combustion, pp 19-22, Indian Institute of Petroleum, Dehradun.
6. Jabez Dhinagar, S., Nagalingam, B. and Gopala Krishnan, K.V., “ Use of alcohol as the sole fuel in an adiabatic diesel engine”, Proceedings of XI National Conference on IC Engines and Combustion, pp: 277-289, I.I.T., Madras, 1989.
7. Parker, D.A. and Dennison, G.M. (1987), The development of an air gap insulated piston”. SAE Paper No. 870652, 1987.
8. Rama Mohan, K., Vara Prasad, C.M. and Murali Krishna, M.V.S. (1999), Performance of a low heat rejection diesel engine with air gap insulated piston, *ASME Journal of Engineering for Gas Turbines and Power*, 121(3), pp 530–540.
9. Vara Prasad, C.M, Murali Krishna, M.V.S., Prabhakar Reddy, C. and Rama Mohan, K. (2000).Performance evaluation of non edible vegetable oils as substitute fuels in low heat rejection diesel engine. *Institute of Engineers (London), 214(2),Part-D, Journal of Automobile Engineering*, pp 181-187.
10. Murali Krishna, M.V.S. (2004). Performance evaluation of low heat rejection diesel engine with alternate fuels. PhD Thesis, J. N. T. University, Hyderabad.
11. **Chennakesava Reddy, Murali Krishna, M.V.S., Murthy, P.V.K., and Ratna Reddy,T. (2011).Potential of low heat rejection diesel engine with crude pongamia oil. *International Journal of Modern Engineering Research*, 1(1), pp *210-224.***
12. Janardhan, N., Murali Krishna, M.V.S., Ushasri, P. and Murthy, P.V.K. (2012). Potential of a medium low heat rejection diesel engine with crude jatropha oil. *International Journal of Automotive Engineering and Technologies, 1(2), pp 1-16*
13. **Murali Krishna, M.V.S., Durga Prasada Rao, N., Anjeneya Prasad, A. and Murthy, P.V.K. (2013). Improving of emissions and performance of rice brawn oil in medium grade low heat rejection diesel engine. *International Journal of Renewable Energy Research*, 3(1), pp 98-108.**
14. **Srikanth, D., Murali Krishna, M.V.S., Ushasri, P. and Krishna Murthy, P.V.(2013), Comparative studies on medium grade low heat rejection diesel engine and conventional diesel engine with crude cotton seed oil, *International Journal of Innovative Research in Science, Engineering and Technology, 2(10), pp 5809-5228.***
15. Fulekar, M. H. (1999). Chemical pollution – a threat to human life, *Indian Journal of Environmental Technology,* 1, pp 353-359.
16. Environmental Pollution Analysis, edited by Khopkar, S.M. (2010). [New Age International (P) Ltd, Publishers, New Delhi], pp 180-190.
17. Engineering Chemistry, edited by Sharma, B.K. (2010). [Pragathi Prakashan (P) Ltd, Meerut], pp 150-160.

International Journal of Engineering Research and General Science Volume 5, Issue 6, November-December, 2017
ISSN 2091-2730

Analysing the Calibration Curve in Different Stage from Project management of Software Development Life Cycle Using Isotonic Regression Classifier

Dr. S.Veni[1], Aparna Srinivasan[2]
[1]Professor and Head: Department of Computer Science
[2]Research Scholar: Department of Computer Science
Karpagam Academy of Higher Education
Karpagam University, Coimbatore, Tamil Nadu, India
research.igate@gmail.com

Abstract— The aim of this research is to identify the deviations from metrics and rectify the deviations using data mining and six sigma techniques. In this research work investigates the effectiveness of using computer-based machine learning algorithms of isotonic regression classifier has to be predicting performance by given data for analyzing the project task of actual and estimated value for planning stage, Designing stage, Building stage, User Acceptance test (UAT) stage, System Integrating Test (SIT) stage, Integration testing and implementation stage in Software Development Life Cycle (SDLC).

Keywords— Isotonic Regression classifier, Calibration curve, Six sigma metrics, project development stages, Pair-adjacent violators algorithm

INTRODUCTION

Using Six Sigma methodology of fig 1 represents the metric to improve the methods by identified and controlled so that there is minimal damage to the project management in SDLC [1] to [3].

Fig 1 Six Sigma metric is to reduce the deviation factor by tracking it from beginning stage of the project

- To predict the success of software projects based on information related to Estimation of planning task and an actual task is deemed to be one of the vital activities in software engineering research.
- The variance is an important metrics parameter which needs to be more focused and optimization of effort and cost variance which gives the significant factor influences internal organization was driven and customer-driven goals based on estimated value and actual value.

SCOPE OF THE RESEARCH

An Isotonic Regression is more powerful when there is sufficient data to prevent from fitting based on Pair-adjacent violators (PAV) algorithm is used to fit the training set according to this mean square error criteria which can analyse by an estimated and actual value of planning, designing and building stage, SIT stage, UAT stage, Integrate testing stage and implementation stage were calibrated at fitted point in the plot.

Table 1 Collections of Qualitative Data and Data Preparation

Stages of development	Sub Attributes
Planning Stage	Estimated Day and Actual day/ Estimated Effort and Actual Effort/ Estimated Cost and Actual Cost
Designing stages	Estimated Day and Actual day/ Estimated Effort and Actual Effort/ Estimated Cost and Actual Cost
Building stages	Estimated Day and Actual day/ Estimated Effort and Actual Effort/ Estimated Cost and Actual Cost
User Acceptance test (UAT) stage	Estimated Day and Actual day/ Estimated Effort and Actual Effort/ Estimated Cost and Actual Cost
System Integrating Test (SIT) stage	Estimated Day and Actual day/ Estimated Effort and Actual Effort/ Estimated Cost and Actual Cost
Integration testing	Estimated Day and Actual day/ Estimated Effort and Actual Effort/ Estimated Cost and Actual Cost
Implementation stage	Estimated Day and Actual day/ Estimated Effort and Actual Effort/ Estimated Cost and Actual Cost

Data collected from an estimated and actual task of each stage of project development as shown in table 1 such as planning , Designing, building, User Acceptance test, System Integrating Test, Integrating test and implementation stages.

An estimated value and actual value parameters of training data set can be analysed by isotonic regression analysis the scheduled for a 50 project task of performance and variance of estimated value for planning stage, Designing stage, Building stage, User Acceptance test (UAT) stage, System Integrating Test (SIT) stage, Integration testing and implementation stage.

RESEARCH METHODOLOGY- ISOTONIC REGRESSION

Isotonic regression depends on the regression metric [4] to [9] and the partially ordered set, an approach using pair adjacent violators (PAV), can be used to determine a non parametric method which leads to a stepwise constant mapping function. This method is more general in that the only restriction is that the mapping function was isotonic and it calibrated predictions from decision trees.

The predictions f_i from a model and the true targets y_i, the basic assumption of Isotonic Regression is that:

$$y_i = h(f_i) + \varepsilon_i \qquad (1)$$

Where h is the isotonic function and ε is an individual error term. A non-decreasing mapping function h can be found given a training set with learned membership values f_i and binary class labels y_i so that h holds the equation of 4.2

$$h = \arg\min_k \sum_{i=1}^{n} (y_i - k(f_i))^2 \qquad (2)$$

Pair-adjacent violators (PAV) algorithm is used to fit the training set according to this mean square error criterion. It has been shown that isotonic regression based calibration using PAV algorithm. A learning curve analysis shows that isotonic regression are prone to over fitting when data is scarce.

EXPERIMENT AND ANALYSIS

From fig 2, represents the schedule, effort and cost actual and predicted fit in the plot. shows the isotonic fit gives a new calibration curve in planning stage of SDLC where the actual value is equal to the estimated value. It may note that the confidence level higher of 99.03 %, it's come out with better estimation, effort and cost task process in maintenance.

From fig 3, represents the schedule, effort and cost actual and predicted fit in the plot. shows the isotonic fit gives a new calibration curve in Designing stage of SDLC where the actual value is predicted from estimated value. It may note that the confidence level higher of 99.01%, it's come out with better estimation, effort and cost task process in maintenance.

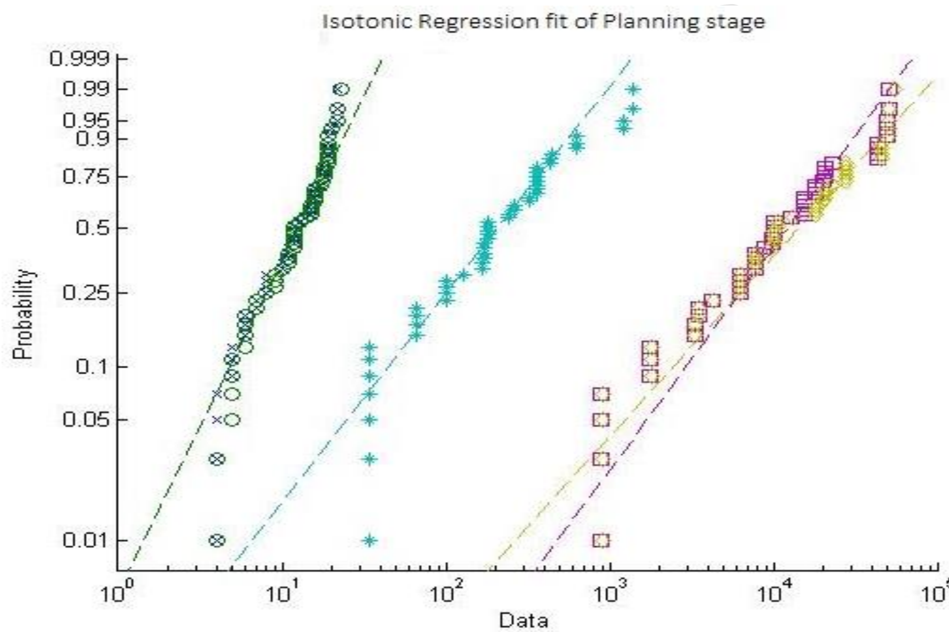

Fig. 2 Calibration curve of planning stage

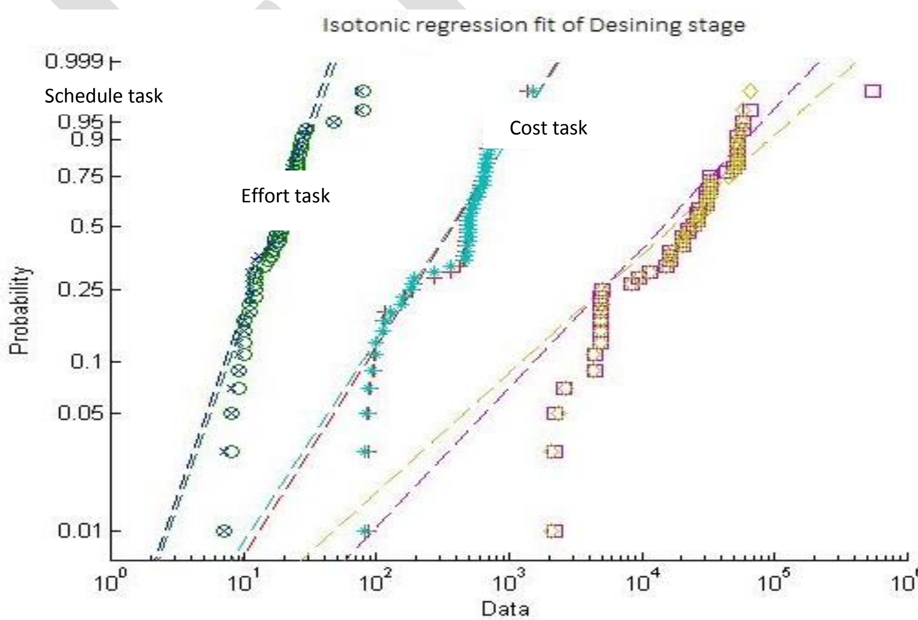

Fig. 3 Calibration curve of Designing stage

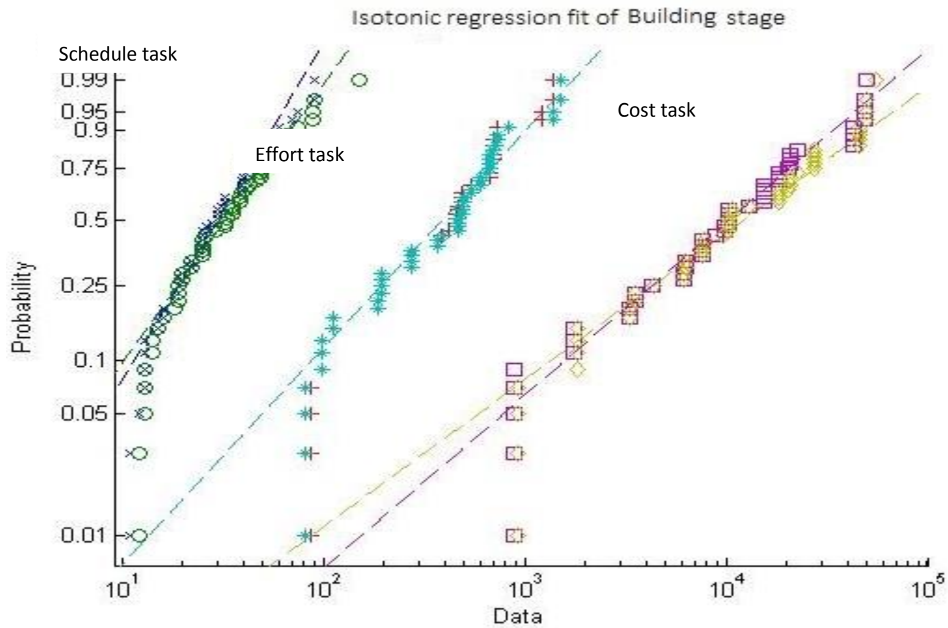

Fig. 4 Calibration curve of Building stage

From fig. 4, represents the schedule, effort and cost actual and predicted fit in the plot. shows the isotonic fit gives a new calibration curve in building stage of SDLC where the actual value is equal to the estimated value. It express goodness of fit well calibrated curves can also indicate the estimation quality. The confidence level is 99.65 %, it's come out with better estimation, effort and cost task process in maintenance.

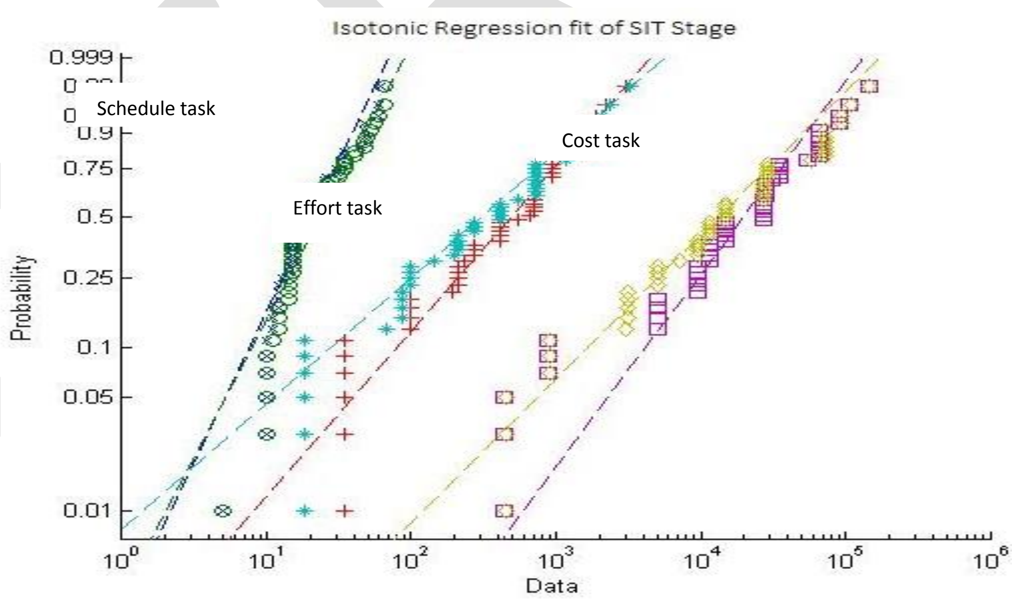

Fig.5 Calibration curve of SIT stage

From fig. 5, represents the schedule, effort and cost actual and predicted fit in the plot. shows the isotonic fit gives a new calibration curve in SIT stage of SDLC where the actual value is equal to the estimated value. It express goodness of fit well calibrated curves can also indicate the estimation quality. The confidence level is 99.79 %, it's come out with better estimation, effort and cost task process in maintenance.

From fig. 6, represents the schedule, effort and cost actual and predicted fit in the plot. shows the isotonic fit gives a new calibration curve in UAT stage of SDLC where the actual value is equal to the estimated value. It express goodness of fit well calibrated curves can also indicate the estimation quality. The confidence level is 99.72 %, it's come out with better estimation, effort and cost task process in maintenance.

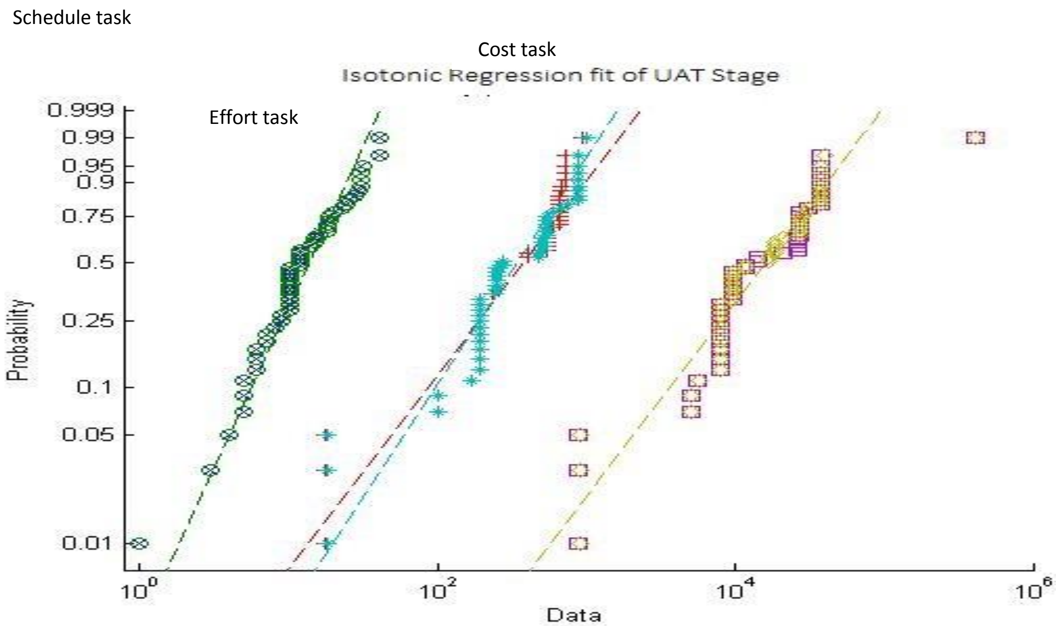

Fig. 6 Calibration curve of UAT stage

From fig. 7, represents the schedule, effort and cost actual and predicted fit in the plot. shows the isotonic fit gives a new calibration curve in integrating testing stage of SDLC where the actual value is equal to the estimated value. It express goodness of fit well calibrated curves can also indicate the estimation quality. The confidence level is 99.70 %, it's come out with better estimation, effort and cost task process in maintenance.

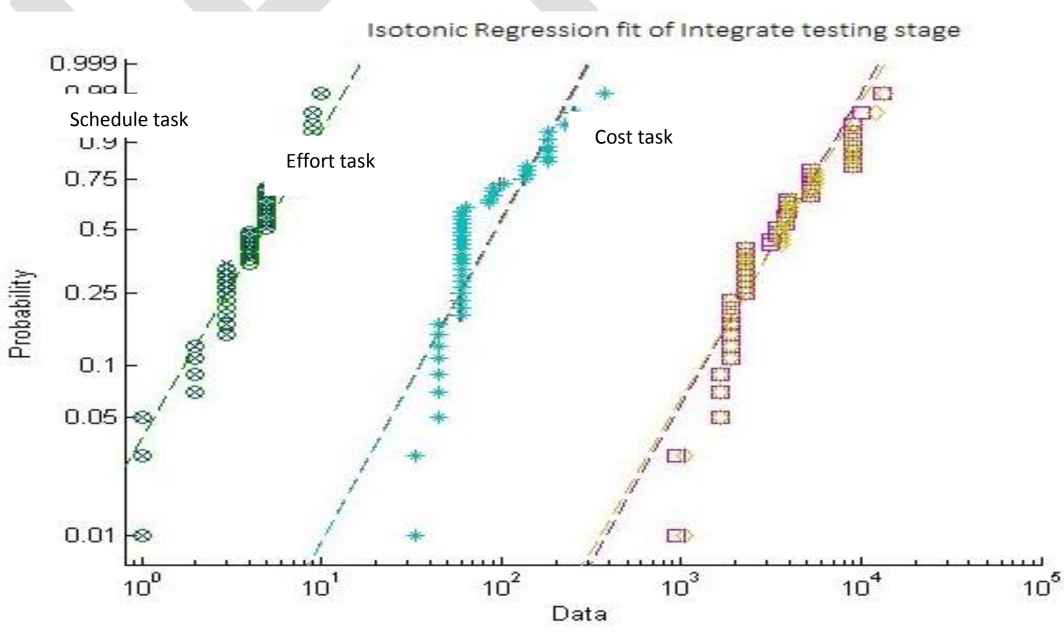

Fig.7 Calibration curve of Integrating Testing stage

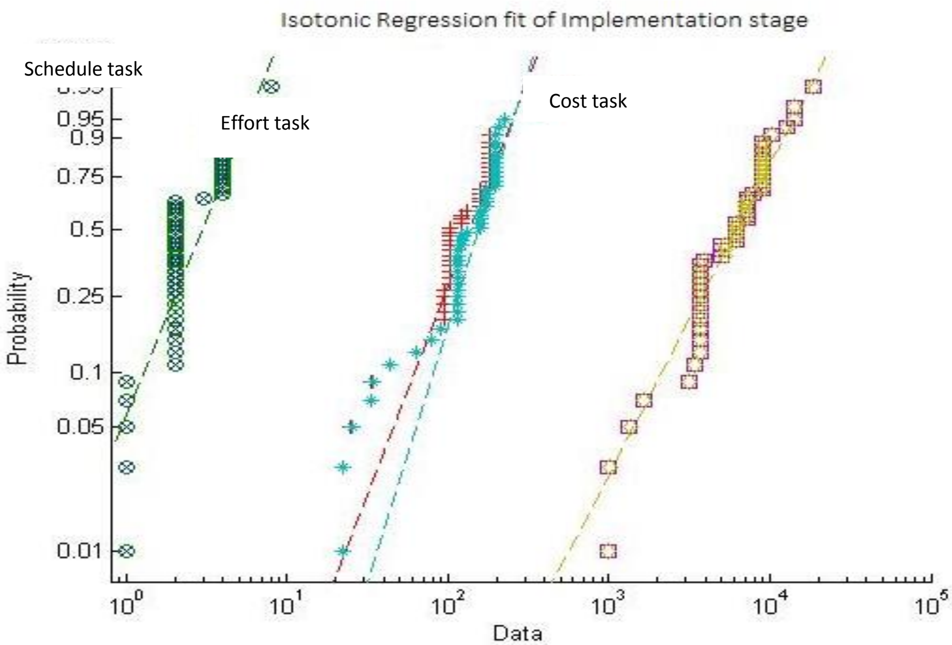

Fig. 8 Calibration curve of Implementation stage

From fig. 8, represents the schedule, effort and cost actual and predicted fit in the plot, shows the isotonic fit gives a new calibration curve in implementation stage of SDLC where the actual value is equal to the estimated value. It express goodness of fit well calibrated curves can also indicate the estimation quality. The confidence level is 99.78 %, it's come out with better estimation, effort and cost task process in maintenance.

CONCLUSION

- In this research work, it can be concluded that an estimated and actual value of planning, designing and building stage are plotted and shown the calibration curve of data points which has fitted in the plot.
- In this research all stage of scheduling day, actual effort and actual cost of software development life cycle represents positively fitted which is a data point above the graph express goodness of fit in the calibration curves.
- Mostly the values are fitted from the plot analyzed as in positive where the data point is above the graph of each stage of the project work. Isotonic Regression is more powerful when there is sufficient data to prevent over fitting based on Pair-adjacent violators (PAV) algorithm is used to fit the training set according to this mean square error criterion.
- From the estimated and actual values are plotted as scatter diagram and isotonic regression analysis is made. It is found that isotonic regression fits for schedule, effort and cost task as well as shown in Fig. 2 to Fig. 8 representing the planning stage, designing stage, building stage, SIT stage, UAT stage, Integrate testing stage and implementation stage.
- An Isotonic regression line shows a new calibrated curve where the actual value is equal to the estimated value which express goodness of fit of the calibration curves can also indicate the estimation quality. The data points fitted positively which can data points above the graph.

REFERENCES:

[1] Stephen H.Kan, “Metrics and Models in Software Quality Engineering”, 2nd edition, , Addison-Wesley, 2003, ISBN 0-201-72915-6.

[2] M. Weske, “Business Process Management: Concepts, Languages, Architectures”. Springer.

[3] William A. Florac and Anita D. Carlton , “Measuring the Software Process: Statistical Process Control for Software Process Improvement", Addison-Wesley, 1999, ISBN 0-201-60444-2.

[4] R. L. Dykstra and T. Robertson. An algorithm for Isotonic Regression for two or more independent variables. The Annals of Statistics, 10(3):pp. 708– 716, 1982.

[5] S. M. Mwagha, M. Muthoni, and P. Ochieg, “Comparison of nearest neighbor (ibk), Regression by discretization and isotonic regression classification algorithms for precipitation classes prediction,” International Journal of Computer Applications, vol. 96, pp. 44-48, 2014.

[6] Han, J. &Kamber, M. (2012). Data Mining: Concepts and Techniques. 3rd.ed. Boston: Morgan Kaufmann Publishers.

[7] Kaner, Cem and Walter P. Bond, Software Engineering Metrics: What Do They Measure and How Do We Know?

[8] Kalai, AT and Sastry, R (2009), “The Isotron algorithm: high-dimensional isotonic regression”, Proc. Comp. Learning Theory (COLT) 2009.

[9] Salanti, G and Ulm, K (2001), “Multidimensional isotonic regression and estimation of the threshold value”, Discussion paper 234, Institute fu¨r Statistik, Ludwig-Maximilians Universita¨t, Munchen.

International Journal of Engineering Research and General Science Volume 5, Issue 6, November-December, 2017
ISSN 2091-2730

Automated Sorting And Grading of Vegetables Using Image Processing

Dr.S.USHA [1], Dr.M.KARTHIK[2], R.JENIFER[3]
[1,2] Associate Professor (Senior Grade),Department of EEE, Kongu Engineering College, India

[3] PG Scholar,Department of EEE, Kongu Engineering College, India

E-mail- jenimerrin@gmail.com [3]

Abstract—The computer vision based system for automatic grading and sorting of agricultural products like strawberry and brinjal based on maturity level is presented in this paper. The application of machine vision based system, aimed to replace manual based technique for grading and sorting of fruit and vegetable. The manual works obtained problems in maintaining consistency in grading and uniformity in sorting. To speed up the process as well as maintain the consistency, uniformity and accuracy, a prototype computer vision based automatic grading and sorting system is developed. The proposed method is implemented by k-means clustering segmentation and color detection process with strawberry and brinjal. Feature extraction for various features like Entropy, Mean and standard deviation are calculated. The main aim of the proposed system is to sort and grade the variety of vegetables like strawberry and brinjal is implemented using image processing techniques. The simulated version of the proposed system is developed using MATLAB R 2013 version and desktop application of the project is developed using MATLAB GUIDE.

Key Words — Sorting, Grading, Kmeans clustering, Feature Extraction and Desktop Applications.

INTRODUCTION

Automated strawberry and brinjal gradation plays an important role to increase the value of produces. In general, the gradation indices are shape, size, color, maturity, defection, etc. With the progress in computer image vision technology, the gradation technique based on computer vision has developed. The computer vision gradation technology is real-time, objective, nondestructive, and can detect multi-index simultaneously, such as size, defection, color, shape and the maturity. There are many reports about qualitative evaluation of agricultural products like In order to determine the influence of mechanical harvest, tomato varieties were mechanical harvested and evaluated in laboratory[1].According to the features citrus fruit can be classified by using GLCM features of the various citrus fruit[2]. Rapid Color Grading for Fruit Quality Evaluation Using Direct Color Mapping[3]color mapping process for various fruit and based upon the color of the gradation process was done. According to the shape, size and color the strawberry can grading by using automation process[4].the apple fruit disease detection was compiled by using segmentation of kmeans clustering segmentation[5]. Estimation of Passion Fruit using Digital Images was implemented[6] according to the mass, volume and artificial neural network is used. Based upon Maturity Prediction System for Sorting of Harvested Mangoes[7] was support vector machine classification. According to the non-destructive quality evaluation[9] was implemented by using image processing with Phyllanthus Emblica(Gooseberry) fruit. From the report of qualitative evaluation of various agricultural products only used one type of fruit and vegetable based upon size, shape, color and their characteristics was done sorting and grading process.

In the paper used the two types fruit used to done the sorting and grading process. The two types are strawberry and brinjal is used to implement the sorting and grading process. The automated strawberry and brinjal sorting, grading system mainly consists of a some simulation process to implement image pre-processing, Histogram equalization, Color detection, segmentation, extracting grading characteristic, desktop application of the project is developed using MATLAB GUIDE. Image noise is defined as distinct pixels which are not similar in appearance with the neighborhood pixels. Over-segmentation occurs mainly due to presence of the noise and unimportant fluctuation which produces non real minima. Main objective of the pre-processing stage is to smooth the original image by removing the noise effect. That noise can be removing by using filters like median filter, Wiener filter and Adaptive filter. After the preprocessing technique next step to implement the histogram equalization. Segmentation process was done by kmeans clustering segmentation. classification was done by various features like entropy, standard deviation and mean based upon the maturity level of strawberry and brinjal.

PROPOSED METHOD

In the proposed system preprocessing, color detection method, and then segmentation process are applied over the image for classification.. The purpose of Preprocessing technique is to remove the noise and enhance the image quality. For removing the noise median filter, wiener filter and adaptive filter are applied finally median filter gave better result compared to wiener and adaptive filter so have to taken the median filter to remove the noise and enhance the image quality. Color detection method demonstrates to the show the affected parts of the fruit by the band, and mask methodology. K-means clustering segmentation is used for the segmentation process. Features extraction was done by three features they are entropy, standard deviation and mean. Figure 1.1 shows the block diagram for the proposed work.

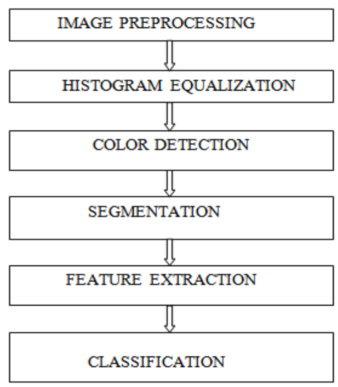

Figure 1.1 Block diagram of Proposed method

1)Preprocessing

In principle, Image noise is defined as distinct pixels which are not similar in appearance with the neighborhood pixels. Over-segmentation occurs mainly due to presence of the noise and unimportant fluctuation which produces non real minima. Main objective of the pre-processing stage is to smooth the original image by removing the noise effect and enhance the image quality of the strawberry and brinjal by using median filter. Median filter is more effective and robust than mean or average filter because a single unrepresentative pixel value in neighborhood affects very less to the median value. Median filter gives one of a neighbor value as an output pixel and hence it does not create new unrealistic values near the edges and preserves sharp edges. It is mathematically expensive to calculate the median value because it requires sorting of nine values for each pixel. Figure 1.2 shows the Concept of Median filter.

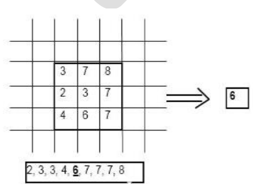

Figure 1.2 Concept of Median Filter

2)Histogram Equalization

The Histogram equalization represents the histogram counts and graphs the total number of pixels at each grayscale level. The output of median is filter is applied to the next step of histogram equalization. From the graph, it can tell whether the strawberry and brinjal image contains distinct regions of a certain gray-level value. A histogram provides a general description of the appearance of an image and helps to identify various components such as the background, objects and noise. The histogram is a fundamental image analysis tool that describes the distribution of the pixel intensities in an image. Use the histogram to determine if the overall intensity in the image is high enough for inspection task. Histogram can be used to determine whether an image contains distinct regions of certain grayscale values. The distinct region of the histogram equalization of the threshold level value for strawberry is 120 similarly threshold level value for the brinjal is 138.

3) Color Detection

The color detection model is used to show the affected part of the fruit by increasing the threshold level value. In this process the red, green, and blue band are applied on the affected fruit image is obtained and then over which the mask like red green and blue is applied. By increasing threshold level for red mask the affected part show the dark one for strawberry image these threshold level is 98. Similarly by increasing threshold level for green mask the affected part show the dark one for brinjal image these threshold level is 70.

4)Segmentation

Image segmentation is process of partitioning the image into multiple segments. In this process Kmeans clustering segmentation is used. The purpose of kmeans clustering segmentation is segmenting the defected part of vegetable and good part of vegetable then find the mean of each cluster.

K-Means is a least-squares partitioning method that divide a collection of objects into K groups. The algorithm iterates over two steps:

1. Compute the mean of each cluster.
2. Compute the distance of each point from each cluster by computing its distance from the corresponding cluster mean. Assign each point to the cluster it is nearest to.
3. Iterate over the above two steps till the sum of squared within group errors cannot be lowered any more.The above three steps was implemented to strawberry and brinjal by using image processing technique.

5) Feature Extraction

The feature extraction is done to measure the maturity level and affected part of strawberry and brinjal. Feature extraction is a method of capturing visual content of an image. The objective of feature extraction process is to represent raw image in its reduced form to facilitate decision making process such as pattern classification. Entropy, Mean and Standard deviation used to extract gradient feature in proposed project. A feature is extracted in order to allow a classifier to distinguish between diseased part and riped fruit.

Image entropy formula is expressed as,

$$\text{Entropy} = -\sum_{i} P_i \operatorname{Log}_2 P_i \qquad \text{.........(1)}$$

Where,

i) Pi is is the probability that the difference between 2 adjacent pixels is equal to i.

ii) Log $_2$ is the base 2 logarithm

The formula for the sample standard deviation is

$$s = \sqrt{\frac{\sum_{i=1}^{N}(x_i - \overline{x})^2}{N-1}}. \qquad \text{...........(2)}$$

Where,

i) N is number of Pixel points

ii) x' is the mean of xi

ISSN 2091-2730

iii) xi is Each values of pixles

The mean is the average of all numbers and is sometimes called the arithmetic mean. The mean formula is expressed as,

$$\overline{X} = \frac{\sum X}{N} \quad \text{............(3)}$$

Where,

i) X' is the mean

ii) N is the number of values

DESKTOP APPLICATIONS

Desktop application was developed by using MATLAB Guide.GUI is expansion of graphical user interface. It is used Create Apps with Graphical User Interfaces in MATLAB. The GUI typically contains controls such as menus, toolbars, buttons, and sliders. Many MATLAB products, such as Curve Fitting Toolbox, Signal Processing Toolbox, and Control System Toolbox include apps with custom user interfaces. The GUI is typically used to develop a desktop applications.

EXPERIMENTAL RESULTS

A. Results for preprocessing technique

The results of preprocessing technique for strawberry and brinjal with various filters shown in Figure 1.3.

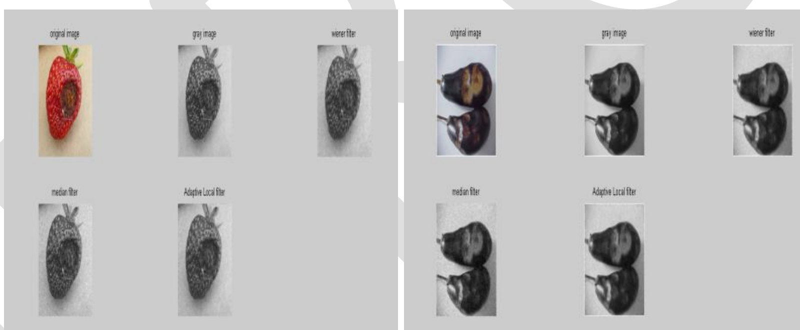

Figure 1.3 Different Filters for strawberry And brinjal

The figure 1.3 refers the various filters applied to the defected strawberry and brinjal finally median filter gave better result to remove noise and enhance image quality.

B. Result for histogram equalization

The Result for histogram equlaization for the strawberry and brinjal shown in figure 1.4 and 1.5.

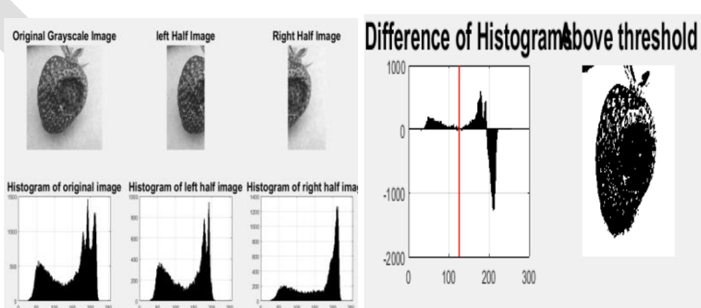

Figure 1.4 Histogram Equalization for strawberry

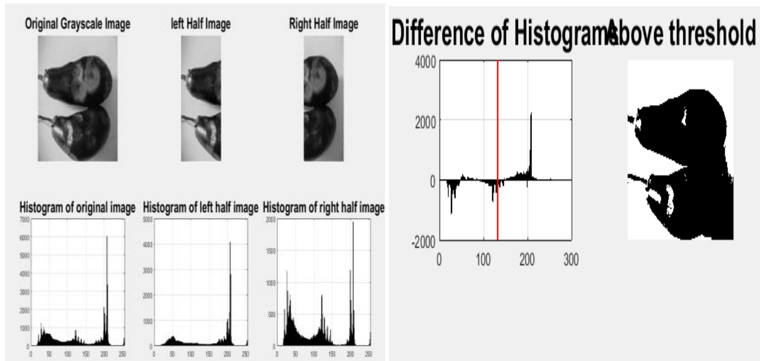

Figure 1.5 Histogram Equalization for brinjal

The figure 1.4 and 1.5 refers the histogram equalization for the defected strawberry and brinjal it gives the threshold level for the distinct regions for strawberry and brinjal.

C. Result for color detection

The experimental result of the color detection for the strawberry and brinjal are shown in figure 1.6 and 1.7

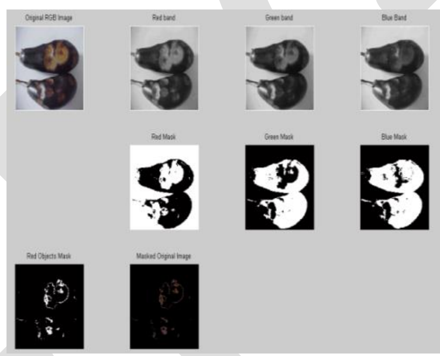

Figure 1.6 Color detection for brinjal

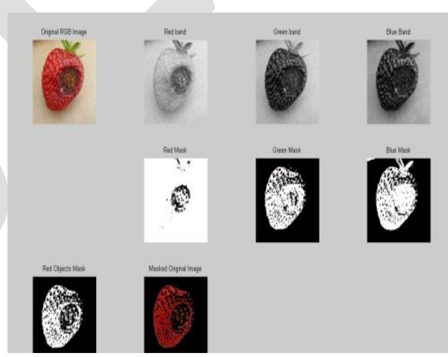

Figure 1.7 Color detection for strawberry

Figure 1.6 and 1.7 refers to show the affected part of strawberry and brinjal by increasing the threshold level value

D. *Result for Segmentation*

The experimental result of the kmeans clustering segmentation for the strawberry and brinjal are shown in figure 1.8 and 1.9.

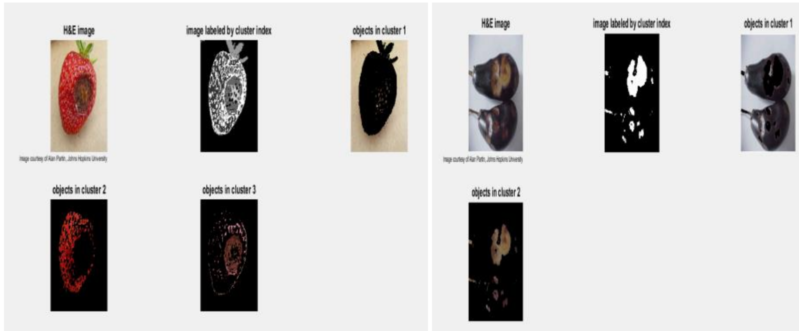

Figure 1.8 Kmeans clustering Segmentation for strawberry and brinjal

Figure 1.8 refers the kmeans clustering segmentation is used segment the defected part and good part of strawberry and brinjal.

E. Result for feature Extraction

The various features like Entrophy, Standard deviation and mean for various maturity level of strawberry and brinjal are shown in Table 1.1,1.2,1.3,1.4.

Table 1.1 Features for Ripe Strawberry Fruit

Entrophy	Standard deviation	Mean	Images
7.497	84.614	155.117	
4.538	83.21	192.66	
5.279	103.289	151.151	

Table 1.1 refers the various the features values for different ripe fruit of strawberry it can be use classify the strawberry and brinjal.

Table 1.2 Features for Unripe Strawberry Fruit

Entropy	SD	Mean	Images
7.78	61.44	104.28	
7.909	69.436	116.929	
7.591	54.45	83.801	

Table 1.2 refers the various feature values for different unripe fruit of strawberry. These features values can be used to classify the strawberry and brinjal.

Table 1.3 Features for Affected Strawberry Fruit

Entropy	SD	Mean	Images
7.649	64.647	142.42	
7.34	85.639	165.79	
5.24	83.811	184.77	

Table 1.3 refers the various feature values for different Affected fruit of strawberry. These features values used to classify the defected fruit and good fruit.

Table 1.4 Features for Various maturity level for Brinjal

Brinjal	Entropy	SD	Mean	Images
Ripe Brinjal	7.507	55.82	109.45	
Unripe Brinjal	7.284	77.62	159.35	
Affected Brinjal	7.346	71.08	125.02	

Table 1.4 refers the various feature values for the ripe, unripe and defected vegetable of brinjal. The features values can be used to classify the different maturity level of strawberry and brinjal.

F. Experimental results for desktop applications

The result of desktop applications using MATLAB GUIDE are shown in figure 1.7.

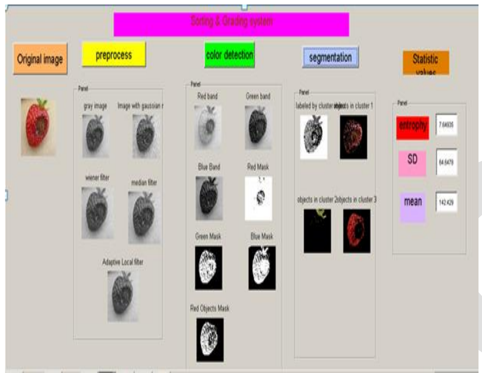

Figure 1.5 Desktop application result for sorting and grading using Strawberry

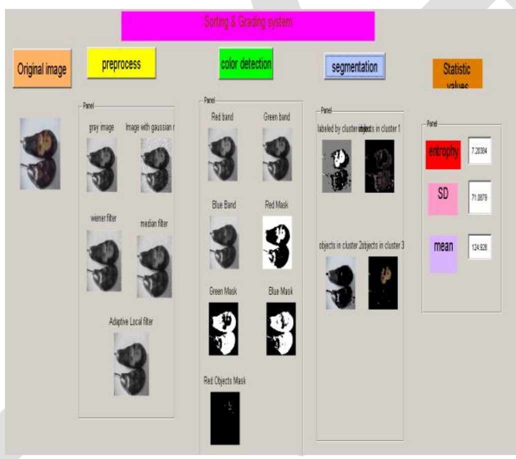

Figure 1.6 Desktop application result for sorting and grading using brinjal

Figure 1.5 and 1.6 refers the desktop application was developed by using MATLAB GUIDE

CONCLUSION

Thus proposed project classify the good and affected fruit of strawberry and brinjal with various techniques. The techniques contains, the preprocessing, Color detection model and segmentation process. The preprocessing technique demonstrates remove the noise and enhance the image quality. When the image is caused by some noise with light intensity or environmental problems to remove those noise by using median filter in this proposed system. Color detection model is used to identify the defected part with the threshold level then the threshold value for strawberry is 98 then threshold level value for brinjal is 70. Then segmentation technique is kmeans clustering segmentation concept this concept split into the different cluster like affected part, non affected part of strawberry and brinjal. After the segmentation process features extraction can be done by the different maturity level of strawberry and brinjal by using various features like entropy, standard deviation and mean. The Various maturity level are Ripe fruit, unripe fruit, affected fruit. Based upon the features values classify the strawberry and brinjal in different maturity level. The whole process is done by simulation in MATLAB and desktop application was developed by using MATLAB GUIDE.

REFERENCES:

[1] S.Arazuri, C.Jaren, J.I.Arana, and J.J.Perez De Ciriza “Influence of Mechanical Harvest on The Physical Properties of Processing Tomato”. Journal of Food Engineering Vol.80(1), pp.190–198,2009.

[2] Chandrankumar, Siddharthchandran, R.Narmathaalla, and Harikamounikagurram “Classifications of Citrus Fruits Using Image Processing GLCM Parameters”. IEEE ICCSP 2015 Conference,2015.

[3] Dah-jye Lee, Jamesk.Arehibald, and Guangingxing(2011) “Rapid Color Grading For Fruit Quality Evaluation Using Direct Color Mapping”. IEEE Transactions on Automation Science and [Engineering, VOL. 8(2), April 2011.

[4] Xu Liming, and Zhaoyancho “Automated Strawberry Grading System Based on Image Processing”. Computers and Electronics in Agriculture71S,pp. S32–S39,2010.

[5] Bhavanij.Samajpati and Sheshangd.Degadwada “Hybrid Approach For Apple Fruit Diseases Detection and Classification Using Random Forest Classifier”.International Conference on Communication and Signal Processing, pp 6-8, April 2016.

[6] J.Bonilla, F.Prieto and C.Perez “Mass and Volume Estimation of Passion Fruit Using Digital Images”. IEEE Latin America Transactions, VOL. 15(2), Feb. 2017.

[7] Chandrasekharnandi, Bipantudu and Chiranjbkoley “A Machine Vision-Based Maturity Prediction System For Sorting of Harvested Mangoes”.IEEE Transactions on Instrumentation and Measurement, VOL 63(7), July 2014.

[8] Monika Jhuria, Ashwanikumar, and Rushikeshborse “Image Procesing for Smart Farming, Detection Disease And Fruit Grading”.Proceedings of The 2013 IEEE Second International Conference on Image Information Processing(ICIIP-2013).

[9] Rohinik.Patel, Kavindrar.Jain, and Tejar.Patel PROPOSED “Non Destructive Quality Evaluation Technique For Processed Phyllanthusemblica (Gooseberry) Using Image Processing”.International Conference on Communication Systems and Network Technologies 2013.

[10] Xu Liming, and Zhaoyancho Proposed “Automatic Fruit Quality Inspection System”. ELSEVIER journal 2010.

International Journal of Engineering Research and general science is an open access peer review publication which is established for publishing the latest trends in engineering and give priority to quality papers which emphasis on basic and important concept through which there would be remarkable contribution to the research arena and also publish the genuine research work in the field of science, engineering and technologies

International Journal Of Engineering Research and General Science
ISSN 2091 - 2730